vaccines

MDPI

Review

Lipid Nanoparticle–mRNA Vaccines for Infectious Diseases: Making a Potent Platform Predictable

Yunwang Zhao [1], Hongxian Cheng [1], Shiyi Zhou [2], Lei He [3], Chenlin Xiu [4], Baihai Huang [4] and Xiongxiong Lu [5,*,†]

[1] Molecular Research and Development Center, Gansu Tianrun Shangjian Medical Technology Co., Ltd., Lanzhou 730000, China; zhaoyunwang1234@163.com (Y.Z.)
[2] Shanghai Weilai Biotechnology Co., Ltd., Shanghai 201315, China; zhoushiyi25@gmail.com
[3] School of Chemistry and Chemical Engineering, Shanghai Jiao Tong University, Shanghai 200240, China
[4] CSPC Megalith Biopharmaceutical Co., Ltd., Shijiazhuang 050025, China
[5] Ruijin Hospital, Shanghai Jiao Tong University School of Medicine, Shanghai 200025, China
* Correspondence: simone515night@126.com
† Affiliation 5 is the primary institution.

Abstract

Lipid nanoparticle (LNP)–mRNA vaccines compressed the path from pathogen sequence to licensed product into less than a year and are now approved for three viral diseases (COVID-19, respiratory syncytial virus and seasonal influenza), with more than twenty indications in clinical development. The platform's potency is no longer in doubt; its predictability is. We argue that progress is now limited by three interfaces that are engineered largely independently: the lipid–RNA interface, which sets encapsulation, internal structure and storage stability; the particle–cell interface, which sets tropism and the efficiency of endosomal escape; and the particle–immune interface, which sets the balance between adjuvanticity and reactogenicity. Quantitative design rules exist for the first interface, remain empirical for the second, and are almost absent for the third, which is why formulation development still proceeds by screening rather than by calculation. We review the molecular design of the mRNA payload and structural antigen selection; the chemistry, manufacture and intracellular trafficking of LNPs; the immunological chain that links innate activation and dendritic-cell cross-presentation to germinal-centre output; and the clinical evidence across COVID-19, respiratory syncytial virus, influenza, cytomegalovirus, HIV, personalised cancer vaccines and other targets. We conclude by identifying the measurements, pharmacopoeial quality attributes and design rules that would make the next generation of LNP–mRNA vaccines predictable rather than empirical.

Keywords: mRNA vaccine; lipid nanoparticle; ionisable lipid; vaccine delivery; germinal centre; pandemic preparedness

Check for updates

Academic Editor: Mariusz Skwarczynski

Received: 19 October 2026
Revised: 6 November 2026
Accepted: 10 November 2026
Published: 19 November 2026

Copyright: © 2026 by the authors. Licensee MDPI, Basel, Switzerland. This article is an open access article distributed under the terms and conditions of the Creative Commons Attribution (CC BY) license.

1. Introduction

Infectious diseases remain a leading cause of death worldwide, and the past two decades have produced a succession of pathogens with pandemic potential, from severe acute respiratory syndrome coronavirus 1 (SARS-CoV-1) in 2002–2003 to pandemic influenza A (H1N1) in 2009, Middle East respiratory syndrome coronavirus (MERS-CoV), Ebola virus, Zika virus in 2015–2016 and SARS-CoV-2 from 2019 onwards [1]. Conventional platforms (live-attenuated, inactivated, protein subunit and viral vector vaccines) typically require five to fifteen years from pathogen identification to licensure, a timescale incompatible with pandemic response [2]. The COVID-19 pandemic showed that mRNA formulated

in lipid nanoparticles (LNPs) could compress that timeline to under twelve months: the first candidate entered phase 1 in March 2020 and emergency use authorisation followed in December 2020 [3,4].

The concept is older than the pandemic. Cationic-liposome-mediated RNA transfection and direct intramuscular injection of naked mRNA were shown to drive protein expression in vivo in 1989–1990 [5,6], and mRNA encoding model viral and tumour antigens elicited cytotoxic T lymphocyte and antibody responses soon afterwards [7,8]. Clinical translation nevertheless stalled for two decades, because unmodified mRNA was unstable and potently immunostimulatory, so that antigen expression was low and variable [9]. Two advances resolved this. Incorporation of naturally occurring modified nucleosides, particularly pseudouridine and N1-methylpseudouridine (m1Ψ), suppressed innate sensing while increasing translation [10], and chromatographic or enzymatic removal of double-stranded RNA (dsRNA) by-products of in vitro transcription removed a second, potent trigger of innate activation [11,12]. In parallel, ionisable lipids designed for small interfering RNA (siRNA) therapeutics were re-engineered for the much larger mRNA cargo [13–15], and the resulting toolkit produced BNT162b2 and mRNA-1273 within a year of the SARS-CoV-2 sequence being released [16,17].

The platform has since diversified across both payload formats and clinical indications. In November 2023, the self-amplifying mRNA (saRNA) vaccine KOSTAIVE (ARCT-154) was approved in Japan for COVID-19 (followed by European Union marketing authorisation), establishing clinical proof of concept for replicating RNA vectors [18]. mRESVIA (mRNA-1345), encoding a prefusion-stabilised respiratory syncytial virus (RSV) F glycoprotein, was approved in May 2024 as the first mRNA vaccine licensed for a disease other than COVID-19 [19], and in August 2026 the US Food and Drug Administration (FDA) approved mFlusiva (mRNA-1010) for seasonal influenza in adults following positive phase 3 efficacy trials [20,21]. Phase 3 programmes now cover pandemic avian influenza (H5N1), combined influenza–COVID-19 vaccination and norovirus, while the pivotal phase 3 CMVictory trial of the hexavalent cytomegalovirus (CMV) candidate mRNA-1647 recently completed readout, and phase 1 and 2 programmes target HIV, Epstein–Barr virus, herpes simplex virus, varicella-zoster virus, Nipah virus, chikungunya and Lyme disease [22]. Beyond infectious diseases, the personalised neoantigen mRNA vaccine intismeran autogene (mRNA-4157) combined with pembrolizumab met its primary phase 3 recurrence-free survival endpoint in resected high-risk melanoma in 2026, further validating the platform's capacity to elicit durable human T cell immunity [23]. The literature has followed: PubMed-indexed records on mRNA vaccines and LNPs rose from essentially none before 2015 to 389 in 2025 (Figure 1). Table 1 summarises the products licensed or authorised to date, together with the efficacy estimates that supported each approval.

This review is organised around a single argument. In 2020, the open question was whether mRNA could be delivered at all; by 2026, it is whether delivery can be made predictable. Three interfaces govern that predictability, and they are currently engineered by different communities using different readouts. The lipid–RNA interface is the most mature: apparent pKa, lipid molar ratio and mixing conditions map onto particle size, encapsulation and internal structure with reasonable reliability. The particle–cell interface is empirical: endosomal escape efficiency is measured retrospectively, if at all, and tropism is directed by library screening rather than by design. The particle–immune interface is the least developed: the same innate activation that supplies intrinsic adjuvanticity drives reactogenicity, and no metric yet predicts where a given formulation will sit on that continuum. Sections 2–4 summarise what is known about each interface, Sections 5–7 review the clinical record and the constraints that surround it, Section 8 sets out the measurements

that would make the platform designable, and Section 9 concludes the paper. Figure 2 places the developments described above in a four-era timeline.

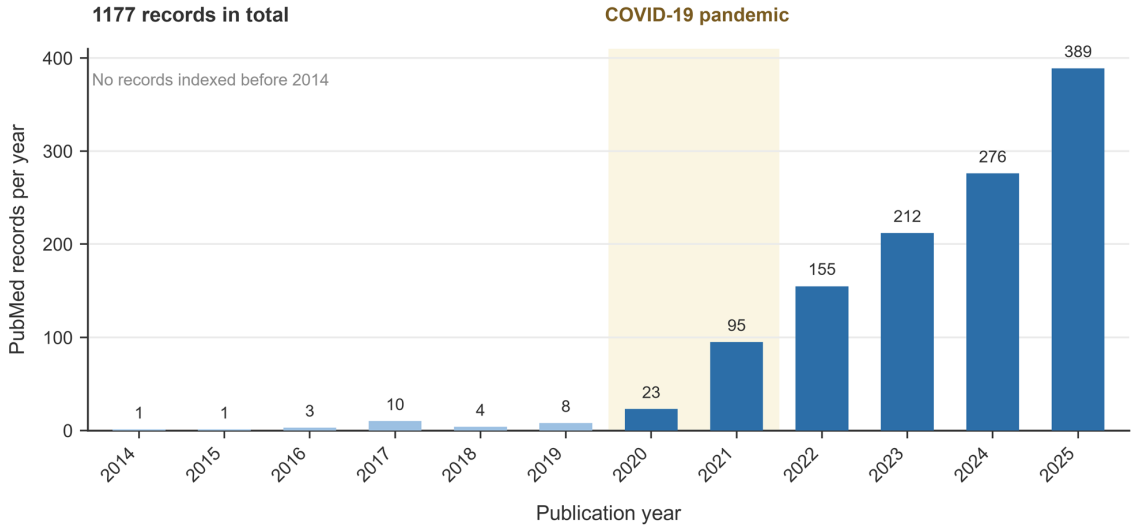


Figure 1. Growth of the LNP–mRNA vaccine literature, 2014–2025. Annual number of PubMed-indexed records retrieved with the query ("mRNA vaccine" OR "messenger RNA vaccine") AND ("lipid nanoparticle" OR LNP); 1177 records in total. No records were indexed before 2014.

Table 1. LNP–mRNA vaccines that are licensed or authorised for human use (status as of late 2026).

Vaccine (Developer)	Indication	mRNA Design	Ionisable Lipid/PEG-Lipid	Efficacy (Pivotal Trial)	Status
BNT162b2/Comirnaty (Pfizer-BioNTech)	COVID-19; updated annually (XBB.1.5, JN.1/KP.2)	m1Ψ-modified, S-2P spike	ALC-0315/ALC-0159	95.0% against symptomatic COVID-19	EUA Dec 2020; FDA approval Aug 2021; >4 billion doses
mRNA-1273/Spikevax (Moderna)	COVID-19; updated annually	m1Ψ-modified, S-2P spike	SM-102/DMG-PEG2000	94.1% against symptomatic COVID-19	EUA Dec 2020; FDA approval Jan 2022
mRNA-1345/mRESVIA (Moderna)	RSV lower-respiratory-tract disease, adults ≥60 years	m1Ψ-modified, prefusion-stabilised F (DS-Cav1)	SM-102/DMG-PEG2000	82.4% against RSV-LRTD (≥2 symptoms)	FDA approval May 2024; first non-COVID mRNA vaccine
KOSTAIVE/ARCT-154 (Arcturus/CSL/Meiji Seika)	COVID-19 (primary series and booster in adults ≥18 years)	Unmodified saRNA (VEEV replicon), S-2P spike	ATX-126/DMG-PEG2000	56.6% against any COVID-19; 95.3% against severe COVID-19; superior booster durability vs. BNT162b2	Japan MHLW approval Nov 2023; EMA approval 2025; first licensed saRNA vaccine [18]
mRNA-1010/mFlusiva (Moderna)	Seasonal influenza (influenza A and B), adults	m1Ψ-modified, quadrivalent haemagglutinin (A/H1N1, A/H3N2, B/Victoria, B/Yamagata)	SM-102/DMG-PEG2000	Superior/non-inferior HAI geometric mean titres; statistically significant phase 3 efficacy confirmed	FDA approval Aug 2026; first licensed mRNA seasonal influenza vaccine [20,21]

Efficacy values are from the pivotal phase 3 trials cited in the text. m1Ψ, N1-methylpseudouridine; S-2P, two-proline prefusion-stabilised spike; LRTD, lower-respiratory-tract disease; saRNA, self-amplifying RNA; VEEV, Venezuelan equine encephalitis virus; HAI, haemagglutination inhibition.

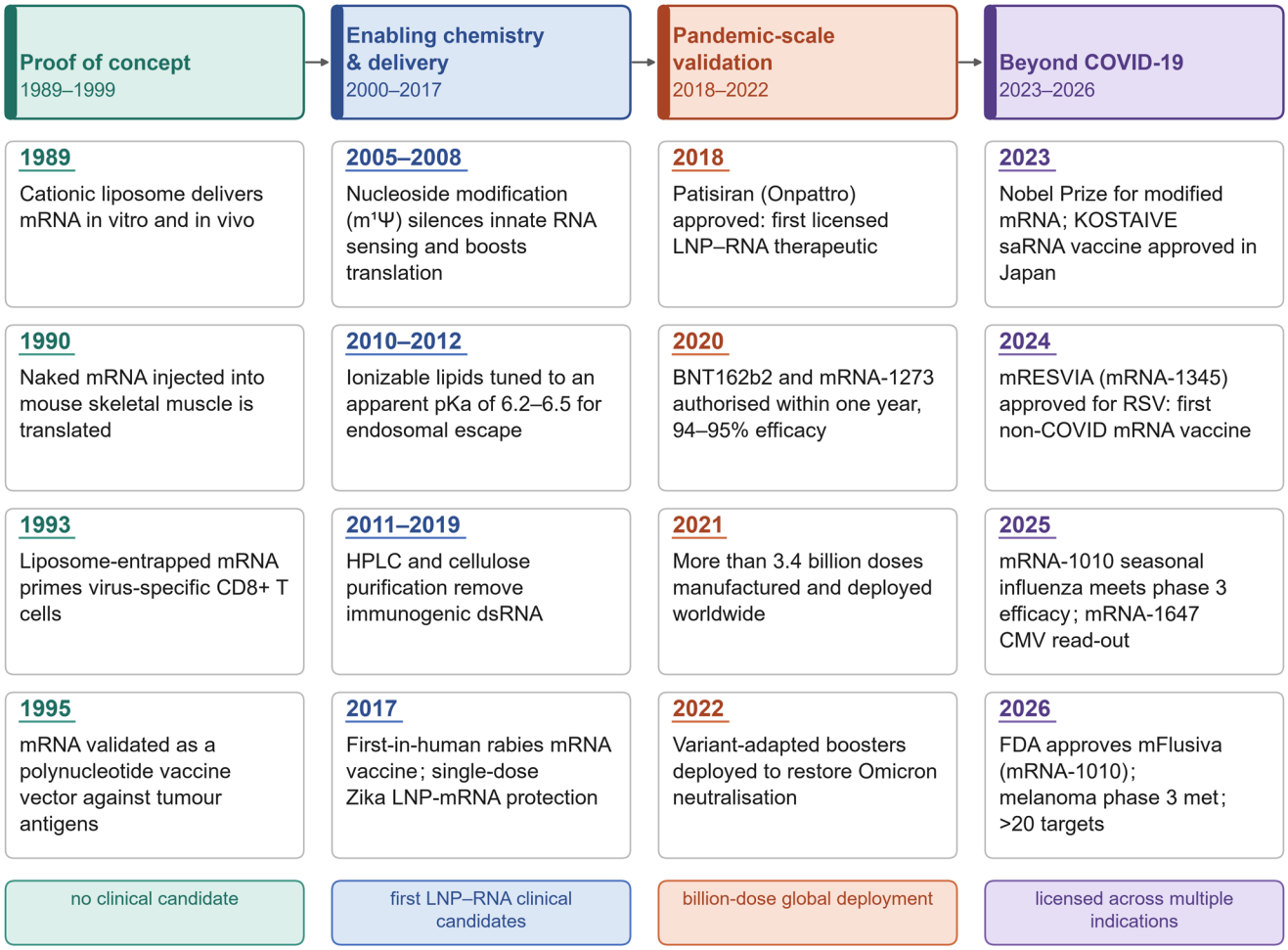


Figure 2. Four eras of LNP–mRNA vaccine development, 1989–2026. Milestones are grouped into proof of concept (1989–1999), enabling chemistry and delivery (2000–2017), pandemic-scale validation (2018–2022) and expansion beyond COVID-19 (2023–2026). Each card gives the year of the primary report or regulatory action together with its corresponding reference citation [3–27]; key clinical milestones include first-in-human rabies mRNA vaccination [24], preclinical Zika virus protection [25], variant-adapted COVID-19 boosters [26], KOSTAIVE saRNA approval [18], mRESVIA RSV approval [19], phase 3 readouts for seasonal influenza (mRNA-1010) [20] and CMV (mRNA-1647) [27], FDA approval of mFlusiva (mRNA-1010) [21], and phase 3 validation of personalised melanoma mRNA vaccination [23]. The strip beneath each column gives the highest level of platform maturity reached in that era.

2. Designing the mRNA Payload

2.1. Sequence Architecture

A vaccine mRNA has five engineered elements: a 5′ cap, a 5′ untranslated region (UTR), the open reading frame, a 3′ UTR and a poly(A) tail [28]. Each is now optimised largely independently. The cap recruits eukaryotic initiation factor 4E and protects the 5′ end from exonucleolytic decay; co-transcriptional capping with cap-1 analogues gives high capping efficiency and avoids the uncapped species that RIG-I recognises as foreign [29]. UTRs set translation efficiency and half-life, and synthetic UTRs selected from cellular libraries outperform the globin-derived sequences used in the first clinical candidates, partly by reducing secondary structure near the initiation codon [29]. Codon choice is a further lever: codon optimality (the match between codon usage and the cellular tRNA pool) rather than GC content per se determines mRNA half-life, and synonymous recoding can change expression several-fold without altering the protein [30,31].

Because these elements interact, combinatorial optimisation of 5′ UTR, coding sequence and 3′ UTR together yields larger gains than sequential optimisation of each, and the design space is now large enough that computational search outperforms intuition [32]. Machine learning has turned this into a generative problem: models trained on random-sequence libraries propose mRNA sequences with improved translational capacity and stability and can be conditioned on cell type or manufacturing constraints [33]. The practical significance is speed. When an antigen must be swapped within weeks, an algorithm that predicts a high-expressing construct from sequence alone removes a round of empirical screening, which is why sequence design has become the part of the platform that iterates fastest.

The poly(A) tail is the least discussed element and the one most easily degraded during manufacture. Its length and homogeneity set both stability and translation, and a short or heterogeneous tail shortens functional half-life in a way that standard integrity assays do not report. Segmented and structured tails are now used to control that decay, and the same logic, namely that secondary structure near the termini governs functional lifetime, has been extended to the coding region, where synonymous recoding can be used deliberately to tune mRNA structure rather than codon usage [31,32].

2.2. Nucleoside Modification and Purity

Unmodified in vitro-transcribed mRNA activates TLR3, TLR7 and TLR8 and the cytosolic sensors RIG-I and MDA5, triggering type I interferon that shuts down translation and can abort expression [9]. Substituting pseudouridine, and more effectively m1Ψ, suppresses this activation while increasing ribosome density and protein output [10,34]. Both licensed COVID-19 vaccines use m1Ψ, and the modification is now a default rather than a choice. Residual dsRNA is the second contaminant of consequence: it is a potent innate agonist at trace levels, and its removal by high-performance liquid chromatography, cellulose purification or RNase III digestion measurably improves expression and tolerability, which is why quantitative measurement of residual dsRNA in the mRNA drug substance is mandated as a critical release attribute and a primary predictor of innate reactogenicity rather than a mere process detail [11,12].

The counter-example is instructive. CureVac's unmodified mRNA vaccine CVnCoV achieved 48% efficacy against COVID-19 in a phase 2b/3 trial, widely attributed to the lower expression and higher innate activation of unmodified mRNA, although dose, antigen and formulation differed as well. The lesson is not that modification is obligatory but that payload chemistry sets the innate set-point, and that the set-point cannot be chosen independently of the formulation. This is the first point at which the three interfaces become coupled, and it recurs throughout this review: a change made to improve one property almost always moves the other two.

2.3. Alternative Formats

Two formats trade payload complexity for dose or durability. Self-amplifying RNA (saRNA) retains the alphavirus non-structural replicase genes, so that a small input is amplified intracellularly; in head-to-head animal studies, it gave protection equivalent to conventional mRNA at doses one to two orders of magnitude lower [35,36], and it has now achieved regulatory licensure with the approval of KOSTAIVE (ARCT-154, zapomeran) against COVID-19 in Japan and the European Union, where a 5 µg saRNA dose elicited higher and more durable neutralising antibody responses than a 30 µg dose of the conventional mRNA vaccine BNT162b2 alongside additional candidates in clinical testing [18,37,38]. The trade-offs are a much larger RNA (typically 9–10 kb, compared with 2–4 kb for conventional mRNA), which constrains encapsulation and manufacturing yield, and replicon-derived dsRNA intermediates that engage innate sensors and can limit

expression. Trans-amplifying designs split the replicon across two molecules to reduce the size of each component, at the cost of a more complex formulation.

Circular RNA closes covalently on itself, resisting exonucleases and permitting cap-independent translation from an internal ribosome entry site [39]. LNP-encapsulated circRNA vaccines encoding SARS-CoV-2 spike elicited durable neutralising antibody responses and protected non-human primates, with better thermostability than linear mRNA [40]. Manufacturing and purification remain the obstacles, and clinical data are still limited, but the format illustrates a general principle: format choice moves the difficulty rather than removing it. saRNA reduces the dose and raises the RNA size; circRNA improves stability and raises the purification burden; neither changes the fact that the particle must still be manufactured, stabilised and delivered.

2.4. Immunogen Design

Before sequence optimisation or LNP formulation can begin, the foundational design decision is selecting which pathogen protein—and in which conformational state—to encode onto the mRNA payload. The sub-year development of the first COVID-19 mRNA vaccines was only possible because nearly two decades of pre-pandemic research on SARS-CoV-1 and MERS-CoV had already established which viral protein generated protective neutralising antibodies [1,41,42]. Specifically, prior coronavirus vaccinology demonstrated that the surface spike (S) glycoprotein, and particularly its receptor-binding domain (RBD) and N-terminal domain, is the principal target of potent neutralising antibodies, whereas immunisation with internal structural proteins such as nucleocapsid (N) failed to confer neutralising protection and risked vaccine-associated enhanced respiratory disease [1,41]. Equally critical was structural engineering of the encoded antigen: studies on RSV F, MERS-CoV S and SARS-CoV-1 S proved that class I viral fusion proteins spontaneously transition from a metastable prefusion trimer to a stable postfusion conformation that displays non-neutralising decoy epitopes [19,41]. The COVID-19 vaccines were therefore as much a triumph of structural antigen selection as of RNA chemistry. The SARS-CoV-2 spike was locked in its prefusion conformation by two consecutive proline substitutions (S-2P) in the central helix, a strategy directly adapted from MERS-CoV and RSV F [41,42]. Prefusion stabilisation preserves the receptor-binding domain and quaternary apex epitopes in the geometry that elicits the most potent neutralising antibodies, and it was adopted in both licensed COVID-19 mRNA vaccines and in mRESVIA, which encodes the DS-Cav1-stabilised RSV F [19]. Where prior antigen biology is less settled, vaccine development is correspondingly slower: for complex herpesviruses such as CMV, protection requires simultaneous targeting of multiple entry pathways—combining the gB fusogen with the pentameric gH/gL/UL128/UL130/UL131 epithelial-entry complex—which requires co-formulating six distinct mRNA species in a single LNP [27]. Breadth is the next objective. A 20-haemagglutinin mRNA cocktail protected against matched and mismatched influenza strains, chimeric spike immunogens elicited pan-sarbecovirus protection in mice, and germline-targeting immunogens are being advanced as mRNA to induce HIV broadly neutralising antibody precursors [43,44]. In each case, the choice and structural engineering of the immunogen, at least as much as the delivery system, is the rate-limiting design problem, which is why the field increasingly treats mRNA as a rapid manufacturing format for antigens that structural and viral immunologists have already solved.

3. The Lipid Nanoparticle

3.1. Composition and Internal Structure

LNPs contain four lipid species: an ionisable lipid, a zwitterionic phospholipid (usually DSPC), cholesterol and a PEG-lipid [45]. The ionisable lipid is the functional core: it complexes the anionic mRNA during formulation, drives endosomal escape after uptake, and is the principal determinant of potency and tolerability [13,46]. DSPC provides bilayer integrity, cholesterol modulates membrane fluidity and stability, and the PEG-lipid sets particle size and shields the surface, with its desorption rate influencing pharmacokinetics [47]. Clinical formulations converge on similar molar ratios, with 46–50% ionisable lipid, 9–10% phospholipid, 38–43% cholesterol and 1.5–2.5% PEG-lipid (Table 2). The convergence is not accidental: the ratio is set by the need for a charge-neutral core at physiological pH and a PEG density low enough to permit cell association.

Table 2. Composition of representative LNP systems and the design parameters that distinguish them.

System	Ionisable Lipid (Apparent pKa)	Helper Lipid	PEG-Lipid	Molar Ratio (Ionisable:Helper:Cholesterol:PEG)	Application
Onpattro (patisiran)	DLin-MC3-DMA (≈6.4)	DSPC	PEG2000-C-DMA	50:10:38.5:1.5	siRNA, hereditary ATTR amyloidosis
BNT162b2	ALC-0315 (≈6.1)	DSPC	ALC-0159	46.3:9.4:42.7:1.6	mRNA vaccine, COVID-19
mRNA-1273/mRNA-1345	SM-102 (≈6.7)	DSPC	DMG-PEG2000	50:10:38.5:1.5	mRNA vaccine, COVID-19 and RSV
C12-200 lipidoid	C12-200	DOPE	C14-PEG2000	35:16:46.5:2.5	Research; siRNA and mRNA
SORT LNP	MC3 plus a SORT lipid	DSPC	DMG-PEG2000	Variable	Tissue-selective mRNA delivery
Adjuvanted-lipid LNP	oLP-05 or lipidoid-A18	DOPE	DMG-PEG2000	Variable	Self-adjuvanted mRNA vaccines

Apparent pKa values are as reported for the formulated particle. Ratios are mol%. ATTR, transthyretin; SORT, selective organ targeting.

The internal architecture is not that of a simple liposome. Cryo-electron microscopy and small-angle X-ray scattering show an electron-dense core of mRNA–ionisable lipid complexes with inverted micellar and lamellar features, surrounded by a lipid envelope decorated with PEG (Figure 3a) [17,48,49]. The balance between a solid core and a more hydrated lamellar interior depends on the drug-to-lipid ratio, pH and mixing, and correlates with transfection potency, a relationship that is reproducible enough to be used as a formulation readout [50]. Recent work has made the structure quantitative, resolving pH-dependent reorganisation of the core during formulation and during endosomal acidification, and linking biophysical parameters to expression [51,52]. Approved particles are 60–100 nm with encapsulation above 90% [16].

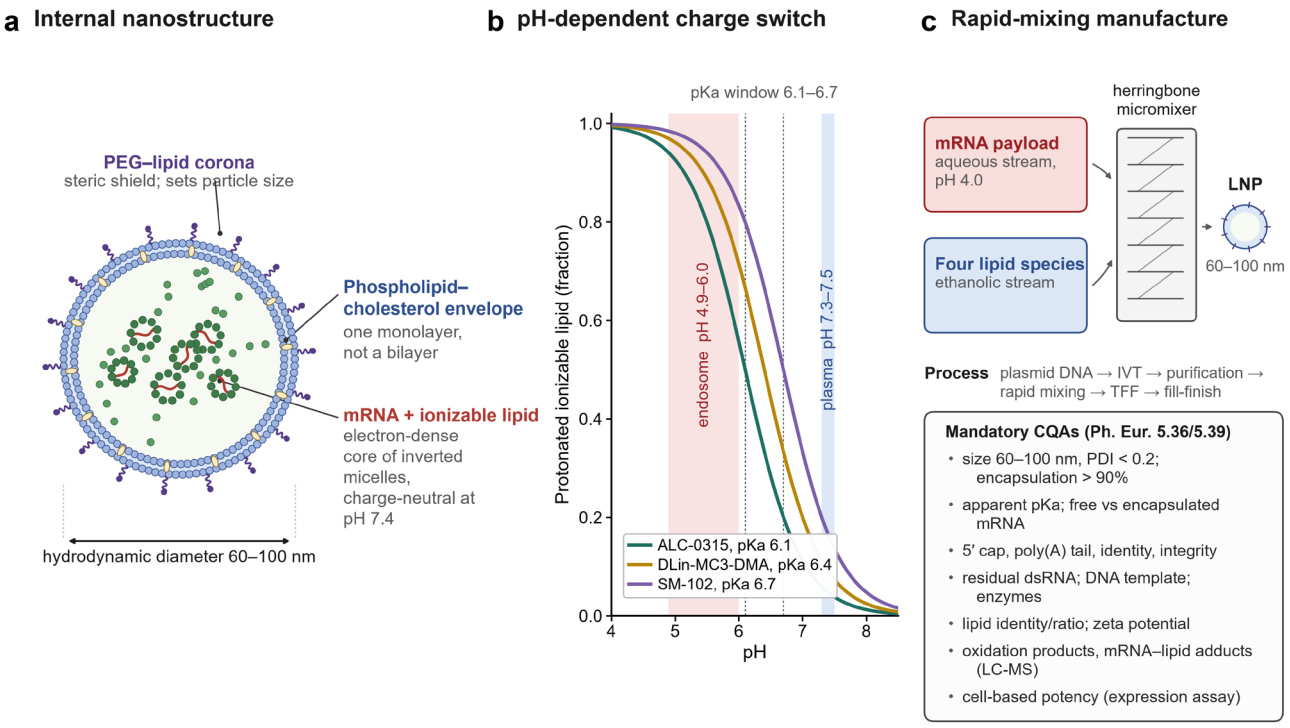


Figure 3. Internal nanostructure, pH-dependent charge switch and manufacture of an LNP–mRNA vaccine (for individual lipid species and molar compositions across systems, see Table 2). (**a**) Schematic cross-section showing an electron-dense core of mRNA complexed with ionisable lipid in inverted micelles, a phospholipid–cholesterol monolayer envelope and a PEG-lipid corona (60–100 nm; encapsulation > 90%). (**b**) Calculated protonated fraction of three representative ionisable lipids, $f = 1/(1 + 10^{(pH-pKa)})$, using the apparent pKa values in Table 2; shading marks the endosomal (pH 4.9–6.0) and plasma (pH 7.3–7.5) ranges. (**c**) Rapid-mixing manufacture and the mandatory critical quality attributes (including Ph. Eur. 5.36/5.39 specifications, lipid oxidation/adducts by LC-MS, and cell-based potency) discussed in the text.

The convergence of composition across companies is itself informative. Ratios that differ by a few per cent behave similarly, whereas the identity of the ionisable lipid changes potency by an order of magnitude, which suggests that the molar ratio is a permissive parameter and the lipid is the determinant one. Formulation development has accordingly shifted from ratio optimisation to lipid discovery, and the screening burden has moved with it.

3.2. Ionisable Lipid Chemistry

The design rule that made the field possible is a pKa window. An ionisable lipid must be neutral at pH 7.4, to avoid nonspecific membrane damage and rapid clearance, and protonated in the endosomal lumen, where it destabilises the bilayer. Titration of a series of amino lipids showed that an apparent pKa between about 6.2 and 6.5 maximises hepatic delivery [14], and the licensed lipids sit in a slightly wider window of 6.1–6.7 (Figure 3b and Table 2). The rule is robust but incomplete: pKa predicts the charge state, not the efficiency with which a given lipid disrupts a given membrane, and lipids with matched pKa can differ by an order of magnitude in potency [46]. The gap between the two is the clearest example of a design rule that is quantitative at the first step and empirical at the second.

It is worth being explicit about what a design rule for this interface would look like, because the field uses the phrase loosely. A rule would take lipid structure and formulation parameters as inputs, predict an apparent pKa and a core morphology, and from those predict encapsulation, size and the fraction of mRNA released in a target cell. Only the first two steps are currently quantitative. The third is where pKa is substituted for mechanism, and where a lipid that titrates correctly but disrupts membranes poorly is predicted to work and does not.

Two structural levers explain much of that residual variation. The first is tail architecture: branched, unsaturated and ester-containing tails tune the cone shape of the molecule and its metabolism, and ester linkers introduce hydrolytic clearance that reduces cumulative exposure and toxicity [53]. The second is head-group chemistry. A systematic comparison showed that amine head groups are themselves sensed, binding TLR4 and CD1d and driving innate responses independently of the RNA cargo [54]. This is a direct link between the lipid–RNA and particle–immune interfaces, and it means that changing the lipid to improve delivery also changes the immunological set-point. Recent series exploit both levers (degradable cyclic amino alcohols that combine potency with rapid clearance, and glutarimide-derived lipids designed for an improved safety and immunogenicity balance [55,56]), while computational screening explores the space more efficiently than rational design [57,58]. The limitation is the objective function: potency in a mouse remains a poor proxy for the human trade-off between titre and reactogenicity.

3.3. Manufacture and Quality Attributes

Manufacturing is a sequence of well-defined unit operations: plasmid template preparation, in vitro transcription, purification including dsRNA removal, LNP formation by rapid mixing of an ethanolic lipid stream with an acidic aqueous mRNA stream, tangential-flow filtration and sterile fill-finish [59]. The mixing step is the critical one. Herringbone micromixers and impingement-jet mixers produce uniform particles by controlling the time scale of nucleation and growth, and parallelised devices allowed the scale-up that made billions of doses possible [60] (Figure 3c). Critical quality attributes (CQAs)—including particle size, polydispersity, encapsulation efficiency, residual dsRNA and ethanol, and lipid identity—are now measured in-process as well as at release [59]. Importantly, batch release and regulatory quality control are now far more comprehensive and legally codified than early pandemic descriptions suggest. The European Pharmacopoeia (Ph. Eur.) Commission has adopted three legally binding general texts governing the quality control of mRNA vaccines in the European Union: mRNA vaccines for human use (general text 5.36), mRNA active substances for the production of mRNA vaccines (5.39), and linear DNA templates used as starting materials (5.40) [61]. These mandatory standards extend well beyond particle size, RNA loading and apparent pKa, requiring rigorous release testing across the DNA template (template purity and linearisation completeness), the mRNA drug substance (sequence identity, 5′ capping efficiency, poly(A) tail length and homogeneity, transcript integrity, residual DNA template, residual enzymatic proteins, and quantitative determination of strongly immunogenic dsRNA impurities), and the formulated LNP drug product (individual lipid identity, content and molar ratio, free versus encapsulated mRNA, particle size distribution, surface charge/zeta potential, pH, osmolality, bacterial endotoxins, sterility, and an in vitro cell-based functional bioactivity/expression assay) [61]. Furthermore, a crucial parameter often omitted from conventional CQA lists is the formation of lipid oxidation products (such as peroxides, reactive aldehydes and tertiary amine N-oxides) in raw or formulated lipids [62]. These oxidative degradants not only act as potent pro-inflammatory triggers that irreversibly heighten clinical reactogenicity without altering apparent pKa or hydrodynamic diameter, but also react covalently with mRNA nucleobases

to generate mRNA–lipid adducts that stall ribosomal translation [62]. Monitoring lipid oxidation species and covalent RNA–lipid adducts via reversed-phase high-performance liquid chromatography coupled with mass spectrometry (RP-HPLC/LC-MS) is therefore essential as a mandatory CQA for both batch release and stability monitoring.

Stability remains the least glamorous constraint and one of the most consequential. Liquid formulations require frozen storage, which shaped the geography of the COVID-19 rollout. Lyophilisation, rigid-core lipid compositions and improved excipients have since produced formulations stable at 2–8 °C, and saRNA or circRNA formats offer further gains [63–65]. The remaining gap is not scientific but economic: a thermostable formulation adds cost per dose, and that cost is borne where cold chains are weakest, which is the subject of Section 7.

3.4. Trafficking and the Escape Ceiling

After intramuscular injection, LNPs enter cells by several routes (clathrin-mediated endocytosis, macropinocytosis and, for some formulations, scavenger-receptor uptake) and are then sorted from early to late endosomes [66]. For systemically administered particles, apolipoprotein E adsorption redirects them to hepatocytes through the LDL receptor, which explains the liver tropism of the siRNA-generation lipids and much of their potency [15]. Endosomal escape is the rate-limiting step. Quantitative imaging of siRNA delivery put escape at 1–2% of the internalised dose, and for mRNA the accepted range is 1–4% [66,67].

That number is quoted so often that its provenance is rarely examined. It derives from a small number of cell types and formulations, measured at fixed time points, and it does not predict expression in vivo. The absence of a quantitative, cell-resolved map of escape is the largest single measurement gap in the field and the reason the particle–cell interface remains empirical. Two strategies compensate. One changes the destination: selective organ targeting adds a fifth lipid that shifts the protein corona and redirects particles to the lungs or spleen, and ionisable phospholipids achieve organ-selective delivery without a targeting ligand [68]. The other adds a ligand, using antibody or peptide display to reach cell types that are otherwise inaccessible [69]. Both work; neither proceeds from a predictive model of where a particle will go, which is why targeting remains a screening problem rather than a design problem.

Two complementary experimental approaches could close the measurement gap. The first uses real-time in situ sensors of endosomal membrane disruption—such as Galectin-8/9-based Förster resonance energy transfer (FRET), fluorescent puncta recruitment or split-luciferase complementation sensors—combined with high-resolution cryo-electron tomography (cryo-ET) and volumetric live-cell imaging, allowing endosomal rupture and tubule-mediated escape to be quantified per cell in real time rather than inferred retrospectively from bulk protein expression [70,71]. The second is orthogonal labelling of the mRNA itself and tracking it through subcellular fractionation, which separates particles that never entered a cell from particles that entered and failed to escape [71]. Neither is yet routine in formulation screening, and neither has been applied systematically across diverse lipid series; that is why the same 1–4% estimate is quoted for formulations that differ by orders of magnitude in potency.

4. Immune Mechanism

4.1. Innate Sensing as Intrinsic Adjuvanticity

An LNP–mRNA vaccine is its own adjuvant. The RNA engages RIG-I, MDA5, PKR and endosomal TLR3, TLR7 and TLR8; the ionisable lipid engages the NLRP3 inflammasome and, through its head group, TLR4 and CD1d; and the combination produces type I interferon together with IL-1, IL-6 and other inflammatory mediators [54,72,73]. The consequence is a paradox that has shaped the field. Type I interferon restricts translation of the delivered mRNA and can abort expression, yet the same signal is required for dendritic-cell maturation, costimulation and the germinal-centre response that produces durable antibody [74]. Adjuvanticity and reactogenicity are therefore not properties of two different components; they are the same property read at different magnitudes (Figure 4d,e).

A second contribution comes from the lipid, and it is easy to overlook because it is not encoded anywhere in the sequence. LNPs containing no RNA still adjuvant a co-administered protein antigen, and ionisable lipids carrying known adjuvant head groups raise the response to encapsidated mRNA above that obtained with the equivalent conventional formulation [74,75]. Part of what is described as the intrinsic adjuvanticity of mRNA vaccines therefore resides in the particle rather than in the payload, which has an immediate consequence: the innate set-point is a property of the formulated product and cannot be inferred from the nucleoside chemistry alone. The two signals also converge intracellularly, since RNA sensing proceeds through RIG-I and MDA5 to MAVS and through endosomal TLRs to MyD88, while the ionisable lipid activates the NLRP3 inflammasome and, for some head groups, TLR4 and CD1d [54,72]. Convergence on a common cytokine output is why altering one component rarely alters one readout.

This is why dose-finding for mRNA vaccines is not a conventional exercise. Increasing the dose raises titre through innate activation and raises reactogenicity through the same pathway, and the therapeutic window is narrow. Two engineering responses follow: remove the innate trigger from the payload and add it back deliberately, through adjuvanted lipids or TLR agonists conjugated into the particle [75], or accept the intrinsic signal and tune its magnitude through lipid chemistry and purification [76]. Neither has yet produced a metric that predicts, for a new formulation, where the optimum will lie.

The dose dependence makes the paradox quantitative. At low doses, interferon induction is transient and acts mainly as an adjuvant signal; at high doses, it becomes a translational brake, so that the same formulation can be dose-limiting for reasons unrelated to its delivery efficiency. This is one reason why potency rankings obtained at a single dose in mice transfer poorly to primates and to humans: the ranking is a property of the dose as much as of the particle.

Species differences make the set-point harder to measure than to describe. Murine TLR8 is not functional, whereas the human receptor responds to RNA degradation products, so the same particle presents a different innate profile in the two species; interferon signalling also differs in amplitude and in the balance of subtypes. Formulations ranked by reactogenicity in mice therefore do not always rank in the same order in primates, and the discrepancy is usually attributed to dose rather than to receptor biology. A set-point metric would have to be defined in a system that reproduces the human receptor repertoire, or calibrated against human data, and no such metric is currently in use [72,76].

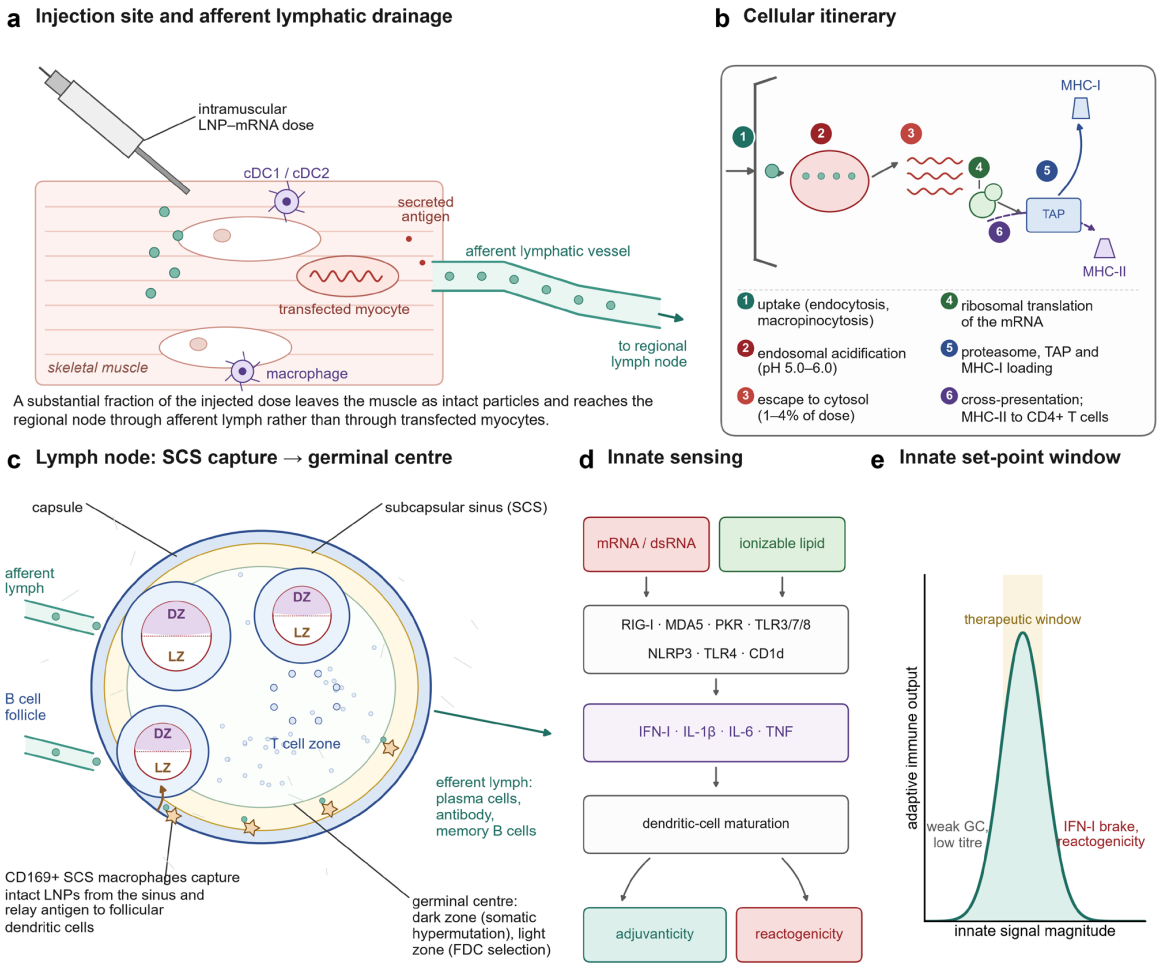


Figure 4. Mechanism of action, from intramuscular injection and afferent lymphatic drainage to germinal-centre output. (**a**) After intramuscular injection, LNPs transfect local myocytes and are taken up by migratory antigen-presenting cells (cDC1, cDC2 and macrophages), while a substantial fraction of intact LNPs drain directly through afferent lymphatic vessels to the regional lymph node. (**b**) Cellular itinerary: 1 endocytosis/macropinocytosis, 2 endosomal acidification, 3 endosomal escape (1–4%), 4 cytosolic ribosomal translation, 5 proteasomal/TAP processing and MHC-I presentation to CD8+ T cells, and 6 exogenous antigen uptake, MHC-II loading and XCR1+ cDC1 cytosolic cross-presentation. (**c**) Draining lymph node, highlighting capture of afferent lymph-borne LNPs by CD169+ subcapsular sinus (SCS) macrophages and resident dendritic cells, antigen relay to follicular dendritic cells (FDCs), B follicles with a germinal centre (dark and light zones), the T cell paracortex, Tfh-B collaboration and the output of long-lived plasma cells, neutralising antibody and memory B cells. (**d**) Innate sensing of the RNA cargo and of the ionisable lipid converges on type I interferon and pro-inflammatory cytokines, which drive dendritic-cell maturation. (**e**) Schematic relationship between the magnitude of the innate signal and the adaptive vaccine response; this panel is conceptual and contains no data.

4.2. Germinal Centres and Durability

The reason two doses of mRNA vaccine induce high titres is that LNPs deliver antigen to germinal centres unusually efficiently. LNP–mRNA drives sustained antigen presentation, strong T follicular helper (Tfh) cell induction and robust germinal-centre B cell responses in mice and macaques, and germinal centres remain detectable in humans for months after immunisation [77,78]. The output (long-lived plasma cells, memory B cells and affinity-matured antibody) determines both peak titre and the slope of decay [79].

Antigen availability and anatomical routing, rather than adjuvant strength alone, set the size and duration of that response. Crucially, a substantial fraction of intramuscularly

injected LNPs do not remain at the injection site to transfect skeletal myocytes; instead, intact 60–100 nm particles rapidly enter afferent lymphatic vessels and drain directly into the subcapsular sinus (SCS) of the regional lymph node (Figure 4a,c) [77,80]. There, draining LNPs are avidly captured by CD169+ SCS macrophages and lymph-node-resident dendritic cells lining the sinus floor, which translate the mRNA payload and relay intact antigen across the sinus floor to cognate B cells and follicular dendritic cells (FDCs) within B cell follicles, while migratory dendritic cells arriving from the muscle sustain antigen input over subsequent days [77,78,80]. Because particulate antigen and persistent mRNA translation supply FDCs continuously for days to weeks, the germinal-centre reaction is sustained rather than transient [77,78]. The same property explains why dose sparing is possible at all, and why the interval between doses matters more for mRNA vaccines than for most adjuvanted proteins. It also defines the measurement problem, because the output of a germinal centre is a function of its duration, and duration cannot be observed in humans without lymph-node fine-needle aspiration. Durability is consequently predicted from serum titres at six months rather than from the lymphoid process that produces them [79].

Durability is nonetheless finite. As observed in the context of SARS-CoV-2 vaccination, neutralising titres fall several-fold within six months, and protection against infection wanes faster than protection against severe disease [81,82]. Two mechanisms complicate updating for rapidly evolving respiratory viruses such as SARS-CoV-2. Antigenic drift erodes neutralisation, as the Omicron lineage demonstrated, and the pace of that drift has not slowed [83,84]. Immune imprinting biases responses towards previously seen epitopes, so that boosters with updated antigens elicit a partly mismatched repertoire [85]. Imprinting is not unique to mRNA vaccines, but it is more visible here, because the platform can update antigen so quickly that the immunological lag, rather than the manufacturing lag, becomes limiting.

4.3. T Cells and Correlates of Protection

mRNA vaccines induce Th1-biased CD4+ T cells and functional CD8+ T cells, with antigen-specific cells detectable years after vaccination [86,87]. Mechanistically, robust CD8+ T cell priming relies on two complementary pathways that bridge exogenous LNP uptake to cytosolic MHC-I loading (Figure 4b) [80,88]. First, when LNPs are internalised by dendritic cells via clathrin-mediated endocytosis or macropinocytosis, protonation of the ionisable lipid in acidifying endosomes (pH 5.0–6.0) destabilises the endosomal membrane and releases mRNA into the cytosol; endogenous ribosomal translation then generates cytosolic protein that is degraded by the proteasome, transported into the endoplasmic reticulum via the transporter associated with antigen processing (TAP), and loaded onto MHC-I molecules [88]. Second, specialised cross-presenting dendritic cell subsets—specifically conventional type 1 dendritic cells (cDC1s, defined by XCR1 and CLEC9A expression) alongside migratory cDC2s—acquire either intact LNPs or antigen secreted and released from transfected myocytes and transfer exogenous protein from endolysosomal compartments into the cytosol for proteasomal MHC-I cross-presentation [80,88]. The physicochemical properties of the LNP directly govern how efficiently these dendritic cell subsets are engaged: particles below 80–100 nm with neutral-to-slightly negative surface charge drain efficiently through afferent lymphatics to reach lymph-node-resident XCR1+ cDC1s, whereas larger or more cationic particles are retained at the injection site and rely on migratory cDC2s; meanwhile, the cone-forming geometry and endosomal membrane-disruption capacity of the ionisable lipid dictate the fraction of internalised mRNA and protein that escapes into the cytosol before lysosomal degradation [80,88]. T cells are less affected by antigenic drift than neutralising antibodies, which is one reason severe-disease protection is more durable than infection protection. For humoral immunity in the context of SARS-CoV-2 vaccines, the

relationship between titre and protection is now quantified well enough to support immunobridging: neutralising titre against the SARS-CoV-2 spike is highly predictive of protection from symptomatic infection, and this relationship has been used to interpret variant-specific and booster data [82,89]. The remaining gap is mucosal immunity. Intramuscular vaccination primes systemic lymphoid organs without imprinting mucosal homing receptors (such as α4β7 integrin or CCR9/CCR10) and consequently produces little respiratory secretory IgA (sIgA) or airway tissue-resident memory T cell response, which limits effects on viral acquisition and transmission, while direct mucosal delivery closes only part of that gap in preclinical models [90,91]. Two fundamental barriers explain why intranasal or inhaled LNP delivery remains difficult to translate [90–92]. The first is biophysical: the respiratory epithelium is coated by a viscoelastic mucus blanket composed of densely glycosylated, negatively charged mucin fibres undergoing continuous mucociliary clearance; conventional LNPs are sterically and electrostatically trapped within this mucin mesh and cleared before they can penetrate to underlying epithelial cells and nasal-associated lymphoid tissue (NALT) dendritic cells [90,92]. Overcoming mucin trapping requires re-engineering the LNP corona (for example, using dense low-molecular-weight PEG, zwitterionic polymers or degradable polymeric carriers) while resisting shear-induced destabilisation during aerosolisation [91,92]. The second barrier is toxicological: cationic and ionisable lipids can provoke acute airway and pulmonary inflammation upon inhalation, and intranasally instilled nanoparticles deposited near the olfactory epithelium can undergo retrograde axonal or perineural transport along the olfactory nerve across the cribriform plate into the olfactory bulb, creating a significant risk of olfactory bulb inflammation, microglial activation and central nervous system neurotoxicity [90,92]. Rigorous exclusion of olfactory-bulb biodistribution and neuroinflammation is therefore a mandatory prerequisite for clinical intranasal LNP formulations.

Correlates of protection are, however, assay-specific in a way that is often glossed over. The titre–protection relationship established for COVID-19 links one neutralisation assay to one clinical endpoint, and it transfers across vaccines because assay and endpoint were held constant, not because neutralisation captures the whole mechanism [82,89]. Where either changes, the threshold does not transfer: protection against RSV lower-respiratory-tract disease is a different endpoint from symptomatic infection, and protection against congenital CMV infection has no established immunological threshold at all. For pathogens for which antibodies are necessary but insufficient, Fc-mediated effector functions and T cell responses will have to enter the correlate, and neither are measured in a standardised way across trials.

4.4. Imprinting and the Limits of Antigen Updating

Updating the antigen is the platform's advertised advantage, and immunology is where that advantage is weakest. As demonstrated in the context of SARS-CoV-2 vaccination and repeated variant boosters, repeated exposure to related SARS-CoV-2 spike antigens drives the response towards epitopes that were immunodominant at first exposure, so that a booster carrying a matched updated sequence still recruits a partly mismatched repertoire; the same mechanism has shaped the convergent evolution of SARS-CoV-2 escape variants [83,85]. The effect is not unique to mRNA vaccines, but the platform makes it visible, because the constraint moves from manufacturing to immunology: a sequence can be designed in weeks and produced in months, whereas the B cell repertoire that will respond to it was fixed years earlier.

Two design strategies are being tested against this. The first changes the immunogen rather than the strain, using germline-targeting immunogens and mosaic or computationally designed trimers to engage naive B cells that current antigens do not reach [43,93,94].

The second changes the schedule, spacing exposures so that earlier germinal centres have resolved before the next antigen arrives. Both require something the field has not yet integrated into routine clinical trial design: a quantitative measurement of the pre-vaccination repertoire and of the epitope bias it imposes, taken before the formulation is chosen rather than after the trial has read out. High-throughput phage immunoprecipitation sequencing (PhIP-Seq) and pan-viral serological profiling platforms such as VirScan—which display proteome-wide peptide tiles across the human viral exposome on bacteriophages to map individual antibody repertoires at epitope resolution—offer a direct technological solution to this bottleneck [95–97]. Incorporating exposome-wide PhIP-Seq profiling prior to immunisation could quantify baseline cross-reactive antibody footprints and historical imprinting hierarchies across cohorts, enabling rational selection of epitope-resurfaced immunogens and adjuvant set-points tailored to pre-existing immunity [96,97].

5. Clinical Translation

5.1. COVID-19

The two pivotal trials set the benchmark: 95% efficacy for BNT162b2 and 94.1% for mRNA-1273 against symptomatic COVID-19 [3,4], with high real-world effectiveness in mass-vaccination settings. Protection was lower against Omicron but remained substantial against severe disease, and boosting restored neutralisation against matched variants [26,83], while the subsequent licensure of the saRNA vaccine KOSTAIVE (ARCT-154) in Japan and Europe demonstrated that replicating RNA formats can extend the duration of neutralising antibody persistence at lower RNA doses [18]. The programme also established population-level safety at a scale no other vaccine platform has matched, and it exposed the two signals (reactogenicity and rare myocarditis) that now define the tolerability agenda.

The practical legacy is less about efficacy than about logistics. Annual antigen updates are now routine, the interval between sequence release and formulated product has fallen to weeks, and the regulatory pathways for strain changes are established. Those are platform properties, and they are the reason influenza and CMV programmes could be designed before the COVID-19 programmes had finished reporting.

A second legacy is regulatory. Once a platform has an approved product, antigen changes can be filed as variations supported by immunogenicity bridging rather than by new efficacy trials, and that pathway, more than the vaccine itself, makes rapid strain updating economically viable. The influenza programme is the first to depend on it, and the CMV programme will test whether bridging also holds for a multivalent antigen.

5.2. Respiratory Syncytial Virus

mRNA-1345 encodes a prefusion-stabilised RSV F and showed 82.4% efficacy against RSV lower-respiratory-tract disease with two or more symptoms in adults aged 60 years and older [19]. Approval in May 2024 made it the first mRNA vaccine licensed for a non-COVID indication and, more importantly, the first test of the platform against a pathogen for which effective adjuvanted protein vaccines already existed. Immunogenicity of revaccination at 12 months has since been reported, addressing the practical question of annual or biennial schedules [98]. The commercial picture is more contested than the clinical one, because the platform must now compete on durability and cost rather than on speed.

5.3. Influenza and Combination Vaccines

Influenza is the most informative test case, because the comparator is a well-established, moderately effective vaccine. Phase 3 trials of mRNA-1010 met their immunogenicity endpoints against influenza A and B strains, eliciting humoral responses that differ qualitatively from those induced by adjuvanted or standard-dose inactivated vaccines, and following

confirmation of clinical efficacy in adults [20,99,100], the US FDA approved mFlusiva (mRNA-1010) in August 2026 as the first licensed mRNA seasonal influenza vaccine [21]. The strategic appeal is manufacturing: a strain update is a sequence change rather than a reassortment and egg-adaptation cycle, which removes a rate-limiting step in the annual campaign.

Combination formulations extend the same logic. Vaccines delivering influenza and SARS-CoV-2 antigens in one injection (such as mRNA-1083) have completed phase 1/2 and phase 3 immunogenicity testing, demonstrating non-inferior or superior humoral responses with acceptable reactogenicity at the doses tested [101,102]. If clinical effectiveness holds, the annual respiratory vaccine could become a single multicomponent product, which would simplify both procurement and delivery.

5.4. Cytomegalovirus

CMV is the hardest target in the current portfolio, because protection requires neutralising antibodies against both the gB fusion protein and the pentameric gH/gL/UL128/UL130/UL131 complex, together with cellular immunity. mRNA-1647 encodes six mRNAs (five forming the pentameric complex and one encoding gB) to cover both arms, and its phase 2 immunogenicity exceeded that of the historic gB/MF59 subunit vaccine, eliciting broader epithelial and fibroblast neutralisation and higher antibody-dependent cellular cytotoxicity [27]. However, topline results from the pivotal phase 3 CMVictory trial (NCT05085366) in seronegative women of childbearing age, reported in late 2025, showed that mRNA-1647 did not meet its primary efficacy endpoint for preventing primary CMV infection (achieving only 6–23% vaccine efficacy across case definitions), leading to discontinuation of the congenital CMV development programme, while phase 2 evaluation continues in haematopoietic stem-cell transplant recipients to suppress viral reactivation. This phase 3 readout is arguably the most instructive immunological data point for the platform since 2020: it demonstrates that generating high systemic neutralising titres against known entry complexes is not by itself sufficient to achieve sterilising mucosal immunity against a latent, immune-evasive herpesvirus, reinforcing the need to pair rational antigen selection with mucosal and Fc-effector correlates of protection.

5.5. HIV and Other Targets

HIV requires induction of broadly neutralising antibodies, which no vaccine has achieved. The germline-targeting approach instead aims to prime rare B cell precursors, and mRNA–LNP delivery of designed trimers and nanoparticles now elicits precursor responses in preclinical models, non-human primates and phase 1 human trials [44,93,94]. Beyond HIV, the preclinical and early clinical portfolio spans Zika, Ebola, Nipah, chikungunya, Lassa, dengue, malaria and norovirus, and mRNA-encoded monoclonal antibodies provide an alternative route to passive protection [25,103,104]. In parallel, the therapeutic oncology milestone achieved in August 2026 by the personalised neoantigen vaccine intismeran autogene (mRNA-4157/V940, encoding up to 34 patient-specific neoantigens) plus pembrolizumab—which significantly improved recurrence-free and distant metastasis-free survival in a phase 3 trial of resected high-risk melanoma [23]—provides critical cross-validation for infectious-disease targets that depend on potent, durable CD8+ and CD4+ T cell immunity. Table 3 summarises the clinical stage of the current pipeline.

Table 3. Selected LNP–mRNA vaccine candidates in clinical development (status as of late 2026).

Indication	Candidate	Sponsor	Phase	Status
COVID-19	BNT162b2; mRNA-1273; KOSTAIVE (ARCT-154)	Pfizer-BioNTech; Moderna; Arcturus/CSL/Meiji	Approved	Annual strain updates since 2022; KOSTAIVE saRNA approved in Japan (2023) and the EU (2025) [18]
RSV	mRNA-1345 (mRESVIA)	Moderna	Approved	Licensed for adults ≥ 60 years; revaccination at 12 months reported
Seasonal influenza	mRNA-1010 (mFlusiva)	Moderna	Approved	Phase 3 immunogenicity and efficacy endpoints met; FDA approved Aug 2026 [20,21]
Influenza + COVID-19	mRNA-1083	Moderna	Phase 3	Multicomponent vaccine; phase 1/2 and phase 3 immunogenicity reported
Pandemic influenza (H5N1)	mRNA-1018	Moderna	Phase 3	Pandemic preparedness against clade 2.3.4.4b
Cytomegalovirus	mRNA-1647 (six antigens)	Moderna	Phase 3 completed/Phase 2 (HSCT)	Phase 2 superior to gB/MF59 [27]; phase 3 CMVictory did not meet primary efficacy endpoint against primary CMV (late 2025); ongoing phase 2 in transplant patients
Norovirus	mRNA-1403	Moderna	Phase 3	Advanced to phase 3 in 2024–2025
HIV	mRNA-1644 (eOD-GT8 60mer)	IAVI/Moderna	Phase 1	Germline-targeting proof of concept
Epstein-Barr virus	mRNA-1189	Moderna	Phase 1	gp350 plus gH/gL
Herpes simplex virus 2	mRNA-1608	Moderna	Phase 1/2	gD plus gC/gE
Varicella-zoster virus	mRNA-1468	Moderna	Phase 1/2	-
Nipah virus	mRNA-1215	NIAID/Moderna	Phase 1	F and G glycoproteins
Zika virus	mRNA-1893	Moderna	Phase 1	prM-E
Lyme disease	mRNA-1975	Moderna	Phase 1/2	OspA
Resected high-risk melanoma (oncology benchmark)	mRNA-4157/V940 (intismeran autogene + pembrolizumab)	Moderna/Merck	Phase 3	Met primary phase 3 endpoint of recurrence-free survival and distant metastasis-free survival (Aug 2026) [23]

6. Safety and Tolerability

The safety database for LNP–mRNA vaccines exceeds that of any previous vaccine platform. Local and systemic reactogenicity is more frequent than after protein or vectored vaccines, is dependent on both dose and dose number, and is consistent with the innate mechanism described above [3,4,73]. It is transient and self-limiting, but it is the main driver of hesitancy in repeated-use settings and the main constraint on dose escalation.

Myocarditis and pericarditis are the signal that matters clinically. Cases cluster in adolescent and young adult males within days of the second dose, at reported rates of roughly 1–10 per 100,000 vaccinated individuals overall and considerably higher in males aged 12–29 years [105,106]. Population-based analyses confirm the association while showing that the absolute risk is low and that SARS-CoV-2 infection carries a substantially higher risk of the same events [107,108]. The mechanism is unresolved; proposed contributors include molecular mimicry with cardiac antigens, LNP-driven innate inflammation and sex-

hormone-dependent immune regulation. Anaphylaxis is rarer still, of the order of 2.5–5 per million doses, and is attributed mainly to the PEG-lipid rather than to the mRNA [109,110].

Three implications follow. First, the myocarditis signal argues for dose and schedule optimisation rather than platform abandonment, and for formulation changes that lower the innate set-point without lowering the germinal-centre response, which is precisely the trade-off the particle–immune interface governs. Second, by late 2026, anti-PEG immunity is no longer viewed merely as a latent concern but is widely recognised across the field as one of the primary limiting factors of the LNP platform for repeated boosting and multi-vaccine regimens [110–112]. Clinical studies have demonstrated that mRNA–LNP vaccination (particularly with mRNA-1273) markedly boosts pre-existing and de novo anti-PEG IgM and IgG titres in humans [111]. Upon subsequent administrations, circulating anti-PEG IgM antibodies bind to the PEGylated nanoparticle surface and trigger the accelerated blood clearance (ABC) phenomenon: complement fixation via the classical and lectin pathways deposits C3b/iC3b opsonins onto the LNP corona, driving rapid phagocytic sequestration by hepatic Kupffer cells and splenic macrophages while simultaneously generating anaphylatoxins (C3a and C5a) that can provoke complement-activation-related pseudoallergy (CARPA) and systemic reactogenicity [110–112]. Third, pregnancy and immunocompromised populations have been studied enough to support clinical use [113,114] but not enough to define optimal booster schedules. Post-authorisation surveillance remains the only mechanism capable of detecting events below 1 in 100,000, and it should be designed as part of the platform rather than appended to it.

Overcoming anti-PEG immunity and the ABC phenomenon has consequently motivated an intensive search for stealth polymer alternatives to PEG-lipids, including polysarcosine (pSar, a non-immunogenic polypeptoid based on endogenous sarcosine), hydrophilic poly(2-oxazoline)s (POx, such as poly(2-ethyl-2-oxazoline) and poly(2-methyl-2-oxazoline)), and zwitterionic or hyperbranched polyglycerol coronas [112,115]. For example, pSar-functionalised LNPs match or exceed the mRNA transfection potency of DMG-PEG2000 formulations while abolishing anti-PEG antibody binding, reducing complement activation and lessening proinflammatory cytokine release upon repeat dosing [115]. Crucially, replacing the hydrophilic corona layer is not a simple one-for-one excipient swap: the chemical identity, chain length, molar density and lipid-anchor desorption kinetics of the stealth polymer directly govern steric hydration, plasma protein adsorption (including apolipoprotein E versus complement and immunoglobulin opsonisation) and receptor-mediated endocytosis, thereby shifting in vivo organ and cellular tropism between muscle, draining lymph nodes, the liver and the spleen [47,112,115]. Designing PEG-free LNPs therefore requires co-optimising the corona polymer alongside the ionisable lipid across all three interfaces.

Two structural changes in preclinical and clinical safety evaluation would accelerate that co-optimisation. First, clinical trials should report solicited local and systemic reactogenicity on a standardised numerical scale alongside the exact mRNA dose, lipid-to-RNA ratio and anti-PEG antibody status, so that the innate set-point becomes a quantitatively comparable property across products rather than an isolated trial observation. Second, the field urgently requires a validated preclinical animal model that faithfully reproduces the human adolescent male myocarditis signal; without one, competing mechanistic hypotheses cannot be falsified prior to large clinical trials, and every novel lipid or corona modification carries an unquantified cardiac risk.

7. Manufacturing, Access and Preparedness

The manufacturing achievement of 2020–2021 is easy to understate. BNT162b2 alone exceeded 4 billion doses within two years, achieved through process intensification, par-

allelised micromixing and rapid construction of new facilities [59,60]. The platform's advantage is that a new antigen requires a sequence change rather than a new cell line, so the same facility can switch product in weeks rather than months [116]. That property is why LNP–mRNA is the central enabling technology of the 100 Days Mission, which aims to deliver a vaccine within 100 days of pathogen identification [117].

Access did not follow scale. Early in the pandemic, more than 80% of doses went to high-income countries, and ultra-cold logistics compounded the disparity [64]. Regional manufacturing, most visibly through the WHO mRNA technology transfer hub in South Africa, is the structural response, and its success depends less on technology transfer than on sustained demand, regulatory capacity and workforce [118]. Thermostable and lyophilised formulations, prefilled devices and simplified release testing are necessary complements [63]. Without them, the platform's speed benefits the countries that need it least, and the next pandemic would reproduce the same asymmetry.

Manufacturing economics are directly coupled to formulation design rather than being a downstream commercial detail. At pandemic scale, the cost of goods per dose for an LNP–mRNA vaccine is driven primarily by raw materials for in vitro transcription (particularly synthetic cap analogues and modified nucleoside triphosphates), GMP synthesis of the ionisable and stealth lipids, and sterile fill-finish and cold-chain distribution. Because the required mass of both mRNA drug substance and lipid excipients scales linearly with the human clinical dose, formulation advances that lower the effective dose without triggering dose-limiting reactogenicity—or that allow storage at 2–8 °C in multi-dose vials—reduce manufacturing cost per dose and expand global production capacity in direct proportion. However, academic formulation screening almost exclusively optimises peak antibody titre in mice rather than minimum effective human dose, thermostability or synthetic simplicity of the lipid, creating a persistent disconnect between laboratory discovery and equitable global access.

8. The Measurement Gap: From Correlation to Prediction

8.1. Why Release Specifications Cannot Predict Immunogenicity

Every licensed LNP–mRNA vaccine is released against a regulatory specification: mRNA integrity above a defined threshold, encapsulation efficiency typically above 90%, a Z-average diameter between 60 and 100 nm, a polydispersity index below 0.2, an apparent pKa in the 6.1–6.7 window, and a defined lipid molar ratio. As codified in the European Pharmacopoeia general texts on mRNA vaccines (5.36, 5.39 and 5.40) [61], mandatory release specifications now also encompass 5′ capping efficiency, poly(A) tail length, quantitative residual dsRNA in the drug substance, lipid-related oxidative impurities and mRNA–lipid covalent adducts measured by LC-MS [62], and in vitro cell-based antigen expression of the formulated drug product. These attributes are necessary conditions for batch-to-batch consistency and safety, and two of them—residual dsRNA in the drug substance and in vitro cell-based bioactivity of the LNP–mRNA drug product—provide direct functional value: dsRNA content sets the baseline innate activation floor [11,12], while cell-based transfection potency in defined target cells serves as a valuable surrogate endpoint for functional batch comparability and for relative ranking of closely related LNP compositions [61]. Even so, release specifications alone are not ab initio in vivo design rules. Two formulations that meet every physicochemical specification can still differ by an order of magnitude in the primate dose required for the same adaptive immune response, as the lipid series that produced the current clinical ionisable lipids demonstrated: apparent pKa and particle size were held nearly constant, while potency in non-human primates moved tenfold [14,46]. Standard release specifications constrain what the product is, not how it traffics across tissues in vivo.

The gap is therefore not a failure of analytics but a mismatch of objectives. Release testing asks whether a batch is what the label says it is. A design rule asks what a formulation will do in a primate at a given dose. The first question can be answered on the batch; the second requires a model linking structure to intracellular fate to immune output, and no such model exists at the accuracy a design decision requires. Table 4 states the requirement in the form in which it would have to be met: for each interface, the property to be predicted, the metric that defines it, the assay that supplies the metric, the current status of that assay, and the threshold the prediction would have to reach.

Table 4. Measurements that would make each interface predictive, with the threshold each would have to reach for a formulation to be designed rather than screened.

Property to Be Predicted	Metric (Definition)	Assay/Measurement	Current Status	Threshold or Target
		Lipid–RNA interface		
RNA loading	Encapsulation efficiency, Z-average diameter, PDI	RiboGreen; dynamic light scattering	Routine, quantitative	≥90%; 60–100 nm; PDI < 0.2
Charge state	Apparent pKa	TNS titration	Quantitative	6.1–6.7
Core structure	Lamellar versus inverse-micellar fraction	SAXS; cryo-EM	Semi-quantitative	A structure–potency map across ≥10 lipid series
Storage stability	Intact mRNA and size drift over time	IP-RP HPLC; light scattering	Measured per product, not predicted	≥24 months at 2–8 °C
Payload and lipid chemical purity (Ph. Eur. CQA)	Residual dsRNA in drug substance; lipid peroxides, aldehydes and mRNA–lipid adducts in drug product	dsRNA-specific ELISA/slot-blot; RP-HPLC and LC-MS/MS [61,62]	Mandated by Ph. Eur. (5.36/5.39); routine for dsRNA, emerging for adducts	dsRNA < 0.01–0.1%; lipid oxidation/adducts below reactogenicity and translation-loss threshold
		Particle–cell interface		
Uptake	Particles or lipid equivalents per cell	Flow cytometry; ICP-MS	Quantitative in vitro	-
Endosomal escape	Fraction of internalised mRNA reaching the cytosol	Cryo-electron tomography (cryo-ET); Galectin-8/9-based FRET or split-luciferase real-time sensors [70,71]; labelled mRNA with subcellular fractionation	Bulk estimates (1–4%)	Cell-resolved, reproducible across ≥3 cell types
In vitro cell-based bioactivity (surrogate potency)	Antigen expression per unit encapsulated mRNA in target cells	Cell-based transfection potency assay (flow cytometry or quantitative ELISA) [61]	Mandatory Ph. Eur. release CQA; routine for relative LNP comparison	Reproducible relative ranking ($R^2 \geq 0.8$) across homologous LNP compositions
Tropism in vivo	Fraction of the dose translated per organ	LNP-Cre reporter mice; organ imaging	Empirical, screening-based	Organ-resolved expression predicted within threefold
Potency	ED50 and expression AUC in primates	Primate dose-ranging	Empirical	Predicted within threefold from lipid structure

Table 4. *Cont.*

Property to Be Predicted	Metric (Definition)	Assay/Measurement	Current Status	Threshold or Target
		Particle–immune interface		
Innate set-point	Type I interferon and IL-1/IL-6 in draining lymph node; coupled to drug-substance dsRNA and lipid head-group/oxidation profile	ELISA, ISG PCR, single-cell RNA-seq	Not standardised	One dose-normalised scalar that predicts reactogenicity
Adjuvanticity	Germinal-centre B cell and Tfh frequency; antigen on FDC	Flow cytometry; confocal microscopy	Quantitative in animals	Adjuvanticity decoupled from reactogenicity
Reactogenicity	Solicited adverse-event grade; fever rate at a given dose	Standardised diary on a common scale	Per product, not comparable	Common scale reported with dose and formulation
Durability	Neutralising titre at 6 and 12 months	Neutralisation assay; node fine-needle sampling	Quantitative; correlate set for COVID-19	Protective titre defined per pathogen
Rare risk	Myocarditis incidence and mechanism	Pharmacovigilance; animal model	Signal only, no model	A validated animal model

Abbreviations: PDI, polydispersity index; TNS, 2-(p-toluidino)naphthalene-6-sulfonate; SAXS, small-angle X-ray scattering; cryo-EM, cryo-electron microscopy; cryo-ET, cryo-electron tomography; FRET, Förster resonance energy transfer; LC-MS/MS, liquid chromatography–tandem mass spectrometry; Ph. Eur., European Pharmacopoeia; IP-RP, ion-pair reversed-phase; AUC, area under the curve; ISG, interferon-stimulated gene; FDC, follicular dendritic cell; Tfh, T follicular helper.

8.2. Three Interfaces, One Measurement Stack

The table is ordered by maturity, and the difference between the blocks is instructive. In the first block, every row is already quantified; what is missing is the mapping from one row to the next, so that a lipid structure and a mixing protocol predict a core morphology and, through it, a stability profile. That mapping is the predictive model of the lipid–RNA interface, and the biophysical tools to build it exist [51,52]. In the second block, the assays exist but are not comparable across studies: while in vitro cell-based expression provides a useful relative surrogate within a homologous series, endosomal escape is typically reported as a bulk fraction for a single immortalised cell line at a fixed time point, and that fraction is then compared across formulations whose in vivo potency differs by two orders of magnitude [66,67,70,71]. In the third block, there is no standardised assay at all, which is why the same mRNA dose can be well tolerated in one product and dose-limiting in another.

The right-hand column is what turns a characterisation into a design rule, and it is the part of the table most likely to be contested. A threshold such as "predicted within threefold from lipid structure" is a claim about the accuracy that a formulation decision requires, not a statistical target; if a model predicts potency to within tenfold, the screen it was meant to replace is still cheaper. The same logic applies to the third interface, where the required output is deliberately stated as a single dose-normalised scalar. Regulators, purchasers and clinicians compare products rather than mechanisms, and a metric that is not scalar cannot enter that comparison. Whether such a scalar can exist is an open question, but the candidate biology is specific: residual dsRNA sensing, lipid head-group sensing through TLR4 and CD1d, the IL-1 axis, and complement activation by the PEG corona each produce a dose-proportional systemic signal that could be calibrated against human reactogenicity data [54,73,75,110,111]. Figure 5 groups the six engineering responses that

these rows imply, and each of them is a candidate intervention on a single row rather than a change of platform.

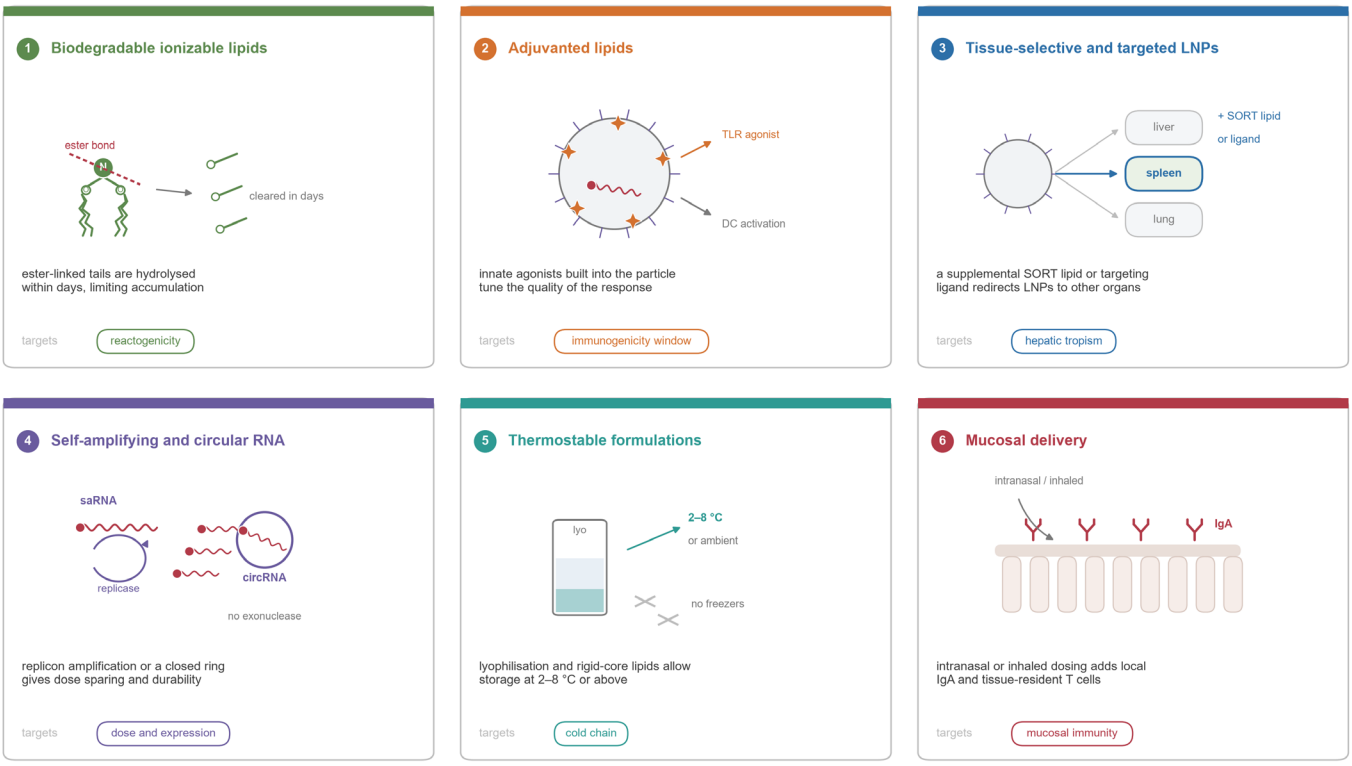


Figure 5. Next-generation engineering strategies. Six approaches that address the challenges discussed in the text: biodegradable ionisable lipids (reactogenicity); adjuvanted lipids (immunogenicity window); tissue-selective and targeted LNPs (hepatic tropism); self-amplifying and circular RNA (dose and durability); thermostable formulations (cold chain); and mucosal delivery (mucosal immunity). Icons are schematic.

Three rows are absent from Table 4 because no candidate metric exists even in principle. The first is batch comparability across manufacturing changes: process transfers and scale changes alter the particle in ways that release specifications do not fully capture, and the clinical consequences are usually discovered in bridging studies rather than predicted [59,60]. The second is the contribution of the device and the injection itself, which sets the local innate environment and is not a property of the formulation. The third is the relationship between the antigen-specific response and the background inflammatory and pre-vaccination repertoire state of the vaccinee, which is large enough to dominate titre variability in older adults and in previously exposed populations [86,87,96].

8.3. Reference Materials, Reporting Standards and Benchmark Sets

A design rule is only as good as the data it is fitted to, and the data in this field are not commensurable. Lipid structures are reported under different nomenclatures; apparent pKa is measured by TNS titration at different lipid concentrations and ionic strengths; mixing is described by flow-rate ratios that do not translate between devices; and dose is expressed variously as total mRNA, encapsulated mRNA or total lipids. A model trained on this literature learns the reporting conventions of its sources as much as the underlying biology [57,58]. The minimum requirement is a reporting checklist covering lipid identity and purity, molar ratios, the pKa method, mixing parameters and device, the encapsulation assay, dose basis and species, and the full set of immunological readouts with their assay platforms.

Beyond reporting, the field needs a benchmark: a small set of formulations characterised by several laboratories with the same assays, in the way that reference materials standardised the measurement of antibody therapeutics. Such a set would do two things that no single laboratory can. It would separate inter-laboratory variance from formulation variance, which is currently inseparable in the published record, and it would supply the negative data that machine-learning approaches lack: published lipid libraries are biased towards compounds that worked, so a model trained on them learns where the cliff is not. Consortia and funders, rather than individual groups, are the plausible owners of such a resource, and the precedent from structural biology—deposition as a condition of publication—is the mechanism most likely to make it used.

8.4. How the Agenda Could Be Tested

A programme of this kind is falsifiable in a specific way, and the test is worth stating before the work is done. Assemble a blinded set of formulations, predict from structure and formulation parameters alone their potency in non-human primates, their organ-resolved expression and their reactogenicity at a fixed dose, and commit to the predictions in advance. Agreement within threefold on potency, and the correct ordering of reactogenicity across ten formulations, would establish that the interfaces are coupled tightly enough to design against. Systematic failure would locate the interface at which the coupling is missing, which is the more useful outcome of the two. That no such formulation exists today, and that candidates are still compared by ranking rather than by calculation, is the evidence for the claim advanced here.

9. Conclusions

Four developments would change the trajectory. The first is a predictive model of the lipid–RNA interface: a quantitative relationship linking lipid structure, apparent pKa and mixing conditions to internal nanostructure, and nanostructure to stability and potency. The biophysical toolkit to build it now exists, and machine-learning-guided lipid design is beginning to supply structure–activity data at the required scale [52,58].

The second is a quantitative, cell-resolved map of endosomal escape and tropism in vivo, enabled by cryo-ET, Galectin-8/9 FRET sensors and standardised cell-based potency assays [70,71]. Without it, targeting remains a screening exercise and the 1–4% escape figure will continue to be quoted without being improved [66,69]. The third is an innate set-point metric: a measurable property of a formulation (integrating residual dsRNA, lipid oxidation impurities and head-group sensing of TLR4 and CD1d alongside anti-PEG corona reactivity) that predicts reactogenicity in humans at a given dose [54,62,75,112]. The fourth is a mucosal formulation engineered to penetrate the respiratory mucin barrier without olfactory-bulb neurotoxicity and tolerable enough for repeated use; without it, the platform will continue to protect primarily against severe disease rather than against mucosal infection [90,92].

None of these is a breakthrough of the kind that nucleoside modification represented, and that is the point. LNP–mRNA vaccines have proved that a synthetic, sequence-defined vaccine can be manufactured at global scale and can protect against a novel pathogen within a year. What remains is to convert an empirically optimised system into a designable one, so that the next formulation, and the next pathogen, do not each require a screening campaign. The clinical pipeline (now encompassing more than twenty indications, licensed vaccines across COVID-19 including the saRNA vaccine KOSTAIVE, RSV with mRESVIA, and seasonal influenza with mFlusiva, instructive phase 3 findings in CMV, and phase 3 clinical validation in melanoma) provides both the motivation and the material for that transition.

Author Contributions: Y.Z.: Writing—original draft, and formal analysis; H.C.: formal analysis and writing—review and editing; S.Z.: visualisation; L.H. and C.X.: methodology and formal analysis; B.H.: conceptualisation; X.L.: writing—review and editing, writing—original draft, methodology, and conceptualisation. All authors have read and agreed to the published version of the manuscript.

Funding: This work was supported in part by the National Natural Science Foundation of China (81560346).

Institutional Review Board Statement: Not applicable.

Informed Consent Statement: Not applicable.

Data Availability Statement: No new data were created or analyzed in this study. Data sharing is not applicable to this article.

Acknowledgments: The authors acknowledge the institutional support of Ruijin Hospital, Shanghai Jiao Tong University School of Medicine, and of the participating institutions.

Conflicts of Interest: Yunwang Zhao and Hongxian Cheng are employees of Gansu Tianrun Shangjian Medical Technology Co., Ltd.; Shiyi Zhou is an employee of Shanghai Weilai Biotechnology Co., Ltd.; Chenlin Xiu and Baihai Huang are employees of CSPC Megalith Biopharmaceutical Co., Ltd. These companies have interests in mRNA vaccine development. Lei He (Shanghai Jiao Tong University) and Xiongxiong Lu (Ruijin Hospital, Shanghai Jiao Tong University School of Medicine) declare no competing interests. The funder had no role in the design of the study, in the interpretation of the literature, or in the decision to publish the results.

Abbreviations

ABC, accelerated blood clearance; AUC, area under the curve; cDC1, conventional type 1 dendritic cell; CMV, cytomegalovirus; cryo-EM, cryo-electron microscopy; cryo-ET, cryo-electron tomography; DLS, dynamic light scattering; dsRNA, double-stranded RNA; ED50, median effective dose; FDC, follicular dendritic cell; FRET, Förster resonance energy transfer; IP-RP, ion-pair reversed-phase; ISG, interferon-stimulated gene; LC-MS, liquid chromatography–mass spectrometry; LNP, lipid nanoparticle; m1Ψ, N1-methylpseudouridine; MHC, major histocompatibility complex; mRNA, messenger RNA; PDI, polydispersity index; PEG, polyethylene glycol; Ph. Eur., European Pharmacopoeia; PhIP-Seq, phage immunoprecipitation sequencing; pKa, negative logarithm of the acid dissociation constant; POx, poly(2-oxazoline); pSar, polysarcosine; SAXS, small-angle X-ray scattering; saRNA, self-amplifying RNA; SCS, subcapsular sinus; siRNA, small interfering RNA; SORT, selective organ targeting; Tfh, T follicular helper; TLR, Toll-like receptor; TNS, 2-(p-toluidino)naphthalene-6-sulfonate; UTR, untranslated region.

References

1. Graham, B.S. Rapid COVID-19 vaccine development. *Science* **2020**, *368*, 945–946. [CrossRef] [PubMed]
2. Pollard, A.J.; Bijker, E.M. A guide to vaccinology: From basic principles to new developments. *Nat. Rev. Immunol.* **2020**, *21*, 83–100, Erratum in *Nat. Rev. Immunol.* **2020**, *21*, 83–100. [CrossRef] [PubMed]
3. Polack, F.P.; Thomas, S.J.; Kitchin, N.; Absalon, J.; Gurtman, A.; Lockhart, S.; Perez, J.L.; Pérez Marc, G.; Moreira, E.D.; Zerbini, C.; et al. Safety and efficacy of the BNT162b2 mRNA COVID-19 vaccine. *N. Engl. J. Med.* **2020**, *383*, 2603–2615. [CrossRef] [PubMed]
4. Baden, L.R.; El Sahly, H.M.; Essink, B.; Kotloff, K.; Frey, S.; Novak, R.; Diemert, D.; Spector, S.A.; Rouphael, N.; Creech, C.B.; et al. Efficacy and safety of the mRNA-1273 SARS-CoV-2 vaccine. *N. Engl. J. Med.* **2021**, *384*, 403–416. [CrossRef] [PubMed]
5. Malone, R.W.; Felgner, P.L.; Verma, I.M. Cationic liposome-mediated RNA transfection. *Proc. Natl. Acad. Sci. USA* **1989**, *86*, 6077–6081. [CrossRef] [PubMed]
6. Wolff, J.A.; Malone, R.W.; Williams, P.; Chong, W.; Acsadi, G.; Jani, A.; Felgner, P.L. Direct gene transfer into mouse muscle in vivo. *Science* **1990**, *247*, 1465–1468. [CrossRef] [PubMed]
7. Martinon, F.; Krishnan, S.; Lenzen, G.; Magné, R.; Gomard, E.; Guillet, J.; Lévy, J.; Meulien, P. Induction of virus-specific cytotoxic T lymphocytes in vivo by liposome-entrapped mRNA. *Eur. J. Immunol.* **1993**, *23*, 1719–1722. [CrossRef] [PubMed]
8. Conry, R.M.; LoBuglio, A.F.; Wright, M.; Sumerel, L.; Pike, M.J.; Johanning, F.; Benjamin, R.; Lu, D.; Curiel, D.T. Characterization of a messenger RNA polynucleotide vaccine vector. *Cancer Res.* **1995**, *55*, 1397–1400. [PubMed]

9. Karikó, K.; Buckstein, M.; Ni, H.; Weissman, D. Suppression of RNA Recognition by Toll-like Receptors: The Impact of Nucleoside Modification and the Evolutionary Origin of RNA. *Immunity* **2005**, *23*, 165–175. [CrossRef] [PubMed]
10. Karikó, K.; Muramatsu, H.; Welsh, F.A.; Ludwig, J.; Kato, H.; Akira, S.; Weissman, D. Incorporation of Pseudouridine Into mRNA Yields Superior Nonimmunogenic Vector With Increased Translational Capacity and Biological Stability. *Mol. Ther.* **2008**, *16*, 1833–1840. [CrossRef] [PubMed]
11. Karikó, K.; Muramatsu, H.; Ludwig, J.; Weissman, D. Generating the optimal mRNA for therapy: HPLC purification eliminates immune activation and improves translation of nucleoside-modified, protein-encoding mRNA. *Nucleic Acids Res.* **2011**, *39*, e142. [CrossRef] [PubMed]
12. Baiersdörfer, M.; Boros, G.; Muramatsu, H.; Mahiny, A.; Vlatkovic, I.; Sahin, U.; Karikó, K. A Facile Method for the Removal of dsRNA Contaminant from In Vitro-Transcribed mRNA. *Mol. Ther. Nucleic Acids* **2019**, *15*, 26–35. [CrossRef] [PubMed]
13. Semple, S.C.; Akinc, A.; Chen, J.; Sandhu, A.P.; Mui, B.L.; Cho, C.K.; Sah, D.W.Y.; Stebbing, D.; Crosley, E.J.; Yaworski, E.; et al. Rational design of cationic lipids for siRNA delivery. *Nat. Biotechnol.* **2010**, *28*, 172–176. [CrossRef] [PubMed]
14. Jayaraman, M.; Ansell, S.M.; Mui, B.L.; Tam, Y.K.; Chen, J.; Du, X.; Butler, D.; Eltepu, L.; Matsuda, S.; Narayanannair, J.K.; et al. Maximizing the Potency of siRNA Lipid Nanoparticles for Hepatic Gene Silencing In Vivo. *Angew. Chem. Int. Ed.* **2012**, *51*, 8529–8533. [CrossRef] [PubMed]
15. Akinc, A.; Maier, M.A.; Manoharan, M.; Fitzgerald, K.; Jayaraman, M.; Barros, S.; Ansell, S.; Du, X.; Hope, M.J.; Madden, T.D.; et al. The Onpattro story and the clinical translation of nanomedicines containing nucleic acid-based drugs. *Nat. Nanotechnol.* **2019**, *14*, 1084–1087. [CrossRef] [PubMed]
16. Hassett, K.J.; Benenato, K.E.; Jacquinet, E.; Lee, A.; Woods, A.; Yuzhakov, O.; Himansu, S.; Deterling, J.; Geilich, B.M.; Ketova, T.; et al. Optimization of Lipid Nanoparticles for Intramuscular Administration of mRNA Vaccines. *Mol. Ther. Nucleic Acids* **2019**, *15*, 1–11. [CrossRef] [PubMed]
17. Schoenmaker, L.; Witzigmann, D.; Kulkarni, J.A.; Verbeke, R.; Kersten, G.; Jiskoot, W.; Crommelin, D.J. mRNA-lipid nanoparticle COVID-19 vaccines: Structure and stability. *Int. J. Pharm.* **2021**, *601*, 120586. [CrossRef] [PubMed]
18. Oda, Y.; Kumagai, Y.; Kanai, M.; Iwama, Y.; Okura, I.; Minamida, T.; Yagi, Y.; Kurosawa, T.; Greener, B.; Zhang, Y.; et al. Immunogenicity and safety of a booster dose of a self-amplifying RNA COVID-19 vaccine (ARCT-154) versus BNT162b2 mRNA COVID-19 vaccine: A double-blind, multicentre, randomised, controlled, phase 3, non-inferiority trial. *Lancet Infect. Dis.* **2023**, *24*, 351–360. [CrossRef] [PubMed]
19. Wilson, E.; Goswami, J.; Baqui, A.H.; Doreski, P.A.; Perez-Marc, G.; Zaman, K.; Monroy, J.; Duncan, C.J.; Ujiie, M.; Rämet, M.; et al. Efficacy and Safety of an mRNA-Based RSV PreF Vaccine in Older Adults. *N. Engl. J. Med.* **2023**, *389*, 2233–2244. [CrossRef] [PubMed]
20. Leroux-Roels, I.; Huang, G.; Ferguson, M.; Kohli, A.; Clark, R.; Bickel, M.; Soens, M.; Du, E.; Pucci, A.; Hicks, B.; et al. Efficacy and Safety of an mRNA Seasonal Influenza Vaccine in Adults. *N. Engl. J. Med.* **2026**, *394*, 1803–1813. [CrossRef] [PubMed]
21. U.S. Food and Drug Administration (FDA). MFLUSIVA (Influenza Vaccine, mRNA-1010) Regulatory Approval and Licens-ing Information. U.S. FDA Biologics Blood & Vaccines 2026. Available online: https://www.fda.gov/vaccines-blood-biologics/vaccines/mflusiva (accessed on 9 November 2026).
22. Parhiz, H.; Atochina-Vasserman, E.N.; Weissman, D. mRNA-based therapeutics: Looking beyond COVID-19 vaccines. *Lancet* **2024**, *403*, 1192–1204. [CrossRef] [PubMed]
23. Fieldhouse, R.; Basu, M. Moderna cancer vaccine stops melanoma returning: What's next for personalized treatments? *Nature* **2026**, *657*, 16–17. [CrossRef] [PubMed]
24. Alberer, M.; Gnad-Vogt, U.; Hong, H.S.; Mehr, K.T.; Backert, L.; Finak, G.; Gottardo, R.; Bica, M.A.; Garofano, A.; Koch, S.D.; et al. Safety and immunogenicity of a mRNA rabies vaccine in healthy adults: An open-label, non-randomised, prospective, first-in-human phase 1 clinical trial. *Lancet* **2017**, *390*, 1511–1520. [CrossRef] [PubMed]
25. Pardi, N.; Hogan, M.J.; Pelc, R.S.; Muramatsu, H.; Andersen, H.; DeMaso, C.R.; Dowd, K.A.; Sutherland, L.L.; Scearce, R.M.; Parks, R.; et al. Zika virus protection by a single low-dose nucleoside-modified mRNA vaccination. *Nature* **2017**, *543*, 248–251. [CrossRef] [PubMed]
26. Garcia-Beltran, W.F.; Denis, K.J.S.; Hoelzemer, A.; Lam, E.C.; Nitido, A.D.; Sheehan, M.L.; Berrios, C.; Ofoman, O.; Chang, C.C.; Hauser, B.M.; et al. mRNA-based COVID-19 vaccine boosters induce neutralizing immunity against SARS-CoV-2 Omicron variant. *Cell* **2022**, *185*, 457–466.e4. [CrossRef] [PubMed]
27. Hu, X.; Karthigeyan, K.P.; Herbek, S.; Valencia, S.M.; Jenks, J.A.; Webster, H.; Miller, I.G.; Connors, M.; Pollara, J.; Andy, C.; et al. Human Cytomegalovirus mRNA-1647 Vaccine Candidate Elicits Potent and Broad Neutralization and Higher Antibody-Dependent Cellular Cytotoxicity Responses Than the gB/MF59 Vaccine. *J. Infect. Dis.* **2024**, *230*, 455–466. [CrossRef] [PubMed]
28. Pardi, N.; Hogan, M.J.; Porter, F.W.; Weissman, D. mRNA vaccines—A new era in vaccinology. *Nat. Rev. Drug Discov.* **2018**, *17*, 261–279. [CrossRef] [PubMed]

29. Orlandini von Niessen, A.G.; Poleganov, M.A.; Rechner, C.; Plaschke, A.; Kranz, L.M.; Fesser, S.; Diken, M.; Löwer, M.; Vallazza, B.; Beissert, T.; et al. Improving mRNA-Based Therapeutic Gene Delivery by Expression-Augmenting 3′ UTRs Identified by Cellular Library Screening. *Mol. Ther.* **2019**, *27*, 824–836. [CrossRef] [PubMed]
30. Presnyak, V.; Alhusaini, N.; Chen, Y.-H.; Martin, S.; Morris, N.; Kline, N.; Olson, S.; Weinberg, D.; Baker, K.E.; Graveley, B.R.; et al. Codon Optimality Is a Major Determinant of mRNA Stability. *Cell* **2015**, *160*, 1111–1124. [CrossRef] [PubMed]
31. Mauger, D.M.; Cabral, B.J.; Presnyak, V.; Su, S.V.; Reid, D.W.; Goodman, B.; Link, K.; Khatwani, N.; Reynders, J.; Moore, M.J.; et al. mRNA structure regulates protein expression through changes in functional half-life. *Proc. Natl. Acad. Sci. USA* **2019**, *116*, 24075–24083. [CrossRef] [PubMed]
32. Leppek, K.; Byeon, G.W.; Kladwang, W.; Wayment-Steele, H.K.; Kerr, C.H.; Xu, A.F.; Kim, D.S.; Topkar, V.V.; Choe, C.; Rothschild, D.; et al. Combinatorial optimization of mRNA structure, stability, and translation for RNA-based therapeutics. *Nat. Commun.* **2022**, *13*, 1536. [CrossRef] [PubMed]
33. Zhang, H.; Liu, H.; Xu, Y.; Huang, H.; Liu, Y.; Wang, J.; Qin, Y.; Wang, H.; Ma, L.; Xun, Z.; et al. Deep generative models design mRNA sequences with enhanced translational capacity and stability. *Science* **2025**, *390*, eadr8470. [CrossRef] [PubMed]
34. Svitkin, Y.V.; Cheng, Y.M.; Chakraborty, T.; Presnyak, V.; John, M.; Sonenberg, N. N1-methyl-pseudouridine in mRNA enhances translation through increased ribosome density. *Nucleic Acids Res.* **2017**, *45*, 6023–6039. [CrossRef] [PubMed]
35. Geall, A.J.; Verma, A.; Otten, G.R.; Shaw, C.A.; Hekele, A.; Banerjee, K.; Cu, Y.; Beard, C.W.; Brito, L.A.; Krucker, T.; et al. Nonviral delivery of self-amplifying RNA vaccines. *Proc. Natl. Acad. Sci. USA* **2012**, *109*, 14604–14609. [CrossRef] [PubMed]
36. Vogel, A.B.; Lambert, L.; Kinnear, E.; Busse, D.; Erbar, S.; Reuter, K.C.; Wicke, L.; Perkovic, M.; Beissert, T.; Haas, H.; et al. Self-Amplifying RNA Vaccines Give Equivalent Protection against Influenza to mRNA Vaccines but at Much Lower Doses. *Mol. Ther.* **2018**, *26*, 446–455. [CrossRef] [PubMed]
37. Pollock, K.M.; Cheeseman, H.M.; Szubert, A.J.; Libri, V.; Boffito, M.; Owen, D.; Bern, H.; McFarlane, L.R.; O'HAra, J.; Lemm, N.-M.; et al. Safety and immunogenicity of a self-amplifying RNA vaccine against COVID-19: COVAC1, a phase I, dose-ranging trial. *eClinicalMedicine* **2022**, *44*, 101262. [CrossRef] [PubMed]
38. Casmil, I.C.; Jin, J.; Won, E.-J.; Huang, C.; Liao, S.; Cha-Molstad, H.; Blakney, A.K. The advent of clinical self-amplifying RNA vaccines. *Mol. Ther.* **2025**, *33*, 2565–2582. [CrossRef] [PubMed]
39. Wesselhoeft, R.A.; Kowalski, P.S.; Anderson, D.G. Engineering circular RNA for potent and stable translation in eukaryotic cells. *Nat. Commun.* **2018**, *9*, 2629. [CrossRef] [PubMed]
40. Qu, L.; Yi, Z.; Shen, Y.; Lin, L.; Chen, F.; Xu, Y.; Wu, Z.; Tang, H.; Zhang, X.; Tian, F.; et al. Circular RNA vaccines against SARS-CoV-2 and emerging variants. *Cell* **2022**, *185*, 1728–1744.e16. [CrossRef] [PubMed]
41. Pallesen, J.; Wang, N.; Corbett, K.S.; Wrapp, D.; Kirchdoerfer, R.N.; Turner, H.L.; Cottrell, C.A.; Becker, M.M.; Wang, L.; Shi, W.; et al. Immunogenicity and structures of a rationally designed prefusion MERS-CoV spike antigen. *Proc. Natl. Acad. Sci. USA* **2017**, *114*, E7348–E7357. [CrossRef] [PubMed]
42. Hsieh, C.-L.; Goldsmith, J.A.; Schaub, J.M.; DiVenere, A.M.; Kuo, H.-C.; Javanmardi, K.; Le, K.C.; Wrapp, D.; Lee, A.G.; Liu, Y.; et al. Structure-based design of prefusion-stabilized SARS-CoV-2 spikes. *Science* **2020**, *369*, 1501–1505. [CrossRef] [PubMed]
43. Arevalo, C.P.; Bolton, M.J.; Le Sage, V.; Ye, N.; Furey, C.; Muramatsu, H.; Alameh, M.-G.; Pardi, N.; Drapeau, E.M.; Parkhouse, K.; et al. A multivalent nucleoside-modified mRNA vaccine against all known influenza virus subtypes. *Science* **2022**, *378*, 899–904. [CrossRef] [PubMed]
44. Leggat, D.J.; Cohen, K.W.; Willis, J.R.; Fulp, W.J.; Decamp, A.C.; Kalyuzhniy, O.; Cottrell, C.A.; Menis, S.; Finak, G.; Ballweber-Fleming, L.; et al. Vaccination induces HIV broadly neutralizing antibody precursors in humans. *Science* **2022**, *378*, eadd6502. [CrossRef] [PubMed]
45. Hou, X.; Zaks, T.; Langer, R.; Dong, Y. Lipid nanoparticles for mRNA delivery. *Nat. Rev. Mater.* **2021**, *6*, 1078–1094. [CrossRef] [PubMed]
46. Sabnis, S.; Kumarasinghe, E.S.; Salerno, T.; Mihai, C.; Ketova, T.; Senn, J.J.; Lynn, A.; Bulychev, A.; McFadyen, I.; Chan, J.; et al. A novel amino lipid series for mRNA delivery: Improved endosomal escape and sustained protein expression. *Mol. Ther.* **2018**, *26*, 1509–1519. [CrossRef] [PubMed]
47. Mui, B.L.; Tam, Y.K.; Jayaraman, M.; Ansell, S.M.; Du, X.; Tam, Y.Y.C.; Lin, P.J.; Chen, S.; Narayanannair, J.K.; Rajeev, K.G.; et al. Influence of Polyethylene Glycol Lipid Desorption Rates on Pharmacokinetics and Pharmacodynamics of siRNA Lipid Nanoparticles. *Mol. Ther. Nucleic Acids* **2013**, *2*, e139. [CrossRef] [PubMed]
48. Arteta, M.Y.; Kjellman, T.; Bartesaghi, S.; Wallin, S.; Wu, X.; Kvist, A.J.; Dabkowska, A.; Székely, N.; Radulescu, A.; Bergenholtz, J.; et al. Successful reprogramming of cellular protein production through mRNA delivered by functionalized lipid nanoparticles. *Proc. Natl. Acad. Sci. USA* **2018**, *115*, E3351–E3360. [CrossRef] [PubMed]
49. Kulkarni, J.A.; Darjuan, M.M.; Mercer, J.E.; Chen, S.; van der Meel, R.; Thewalt, J.L.; Tam, Y.Y.C.; Cullis, P.R. On the Formation and Morphology of Lipid Nanoparticles Containing Ionizable Cationic Lipids and siRNA. *ACS Nano* **2018**, *12*, 4787–4795. [CrossRef] [PubMed]

50. Carrasco, M.J.; Alishetty, S.; Alameh, M.-G.; Said, H.; Wright, L.; Paige, M.; Soliman, O.; Weissman, D.; Cleveland, T.E.; Grishaev, A.; et al. Ionization and structural properties of mRNA lipid nanoparticles influence expression in intramuscular and intravascular administration. *Commun. Biol.* **2021**, *4*, 956. [CrossRef] [PubMed]
51. Guruge, A.G.; He, Y.; Clulow, A.J.; Pouton, C.W.; Chalmers, D.K. Structuring of lipid nanoparticle mRNA formulations at acidic and neutral pH: X-ray scattering and molecular dynamics studies. *Mol. Ther. Methods Clin. Dev.* **2025**, *33*, 101596. [CrossRef] [PubMed]
52. Padilla, M.S.; Shepherd, S.J.; Hanna, A.R.; Kurnik, M.; Zhang, X.; Chen, M.; Byrnes, J.; Joseph, R.A.; Yamagata, H.M.; Ricciardi, A.S.; et al. Elucidating lipid nanoparticle properties and structure through biophysical analyses. *Nat. Biotechnol.* **2026**, *44*, 1502–1515. [CrossRef] [PubMed]
53. Maier, M.A.; Jayaraman, M.; Matsuda, S.; Liu, J.; Barros, S.; Querbes, W.; Tam, Y.K.; Ansell, S.M.; Kumar, V.; Qin, J.; et al. Biodegradable Lipids Enabling Rapidly Eliminated Lipid Nanoparticles for Systemic Delivery of RNAi Therapeutics. *Mol. Ther.* **2013**, *21*, 1570–1578. [CrossRef] [PubMed]
54. Chaudhary, N.; Kasiewicz, L.N.; Newby, A.N.; Arral, M.L.; Yerneni, S.S.; Melamed, J.R.; LoPresti, S.T.; Fein, K.C.; Petersen, D.M.S.; Kumar, S.; et al. Amine headgroups in ionizable lipids drive immune responses to lipid nanoparticles by binding to the receptors TLR4 and CD1d. *Nat. Biomed. Eng.* **2024**, *8*, 1483–1498. [CrossRef] [PubMed]
55. Rudra, A.; Gupta, A.; Reed, K.; Deik, A.; Min, J.; Mansour, H.M.A.; Nguyen, Q.T.C.; Danko, A.; Hu, Y.; Berger, A.; et al. Degradable cyclic amino alcohol ionizable lipids as vectors for potent influenza mRNA vaccines. *Nat. Nanotechnol.* **2025**, *20*, 1831–1842. [CrossRef] [PubMed]
56. Li, S.; Zheng, L.; Zhang, Z.; Zhang, J.; Liu, X.; Xu, J.; Yang, R.; Yang, Y.; Zhao, Y.; Zhong, J.; et al. Glutarimide-derived ionizable lipid enables mRNA lipid nanoparticle vaccines with enhanced safety and immunogenicity. *J. Control. Release* **2025**, *389*, 114482. [CrossRef] [PubMed]
57. Han, X.; Zhang, H.; Butowska, K.; Swingle, K.L.; Alameh, M.G.; Weissman, D.; Mitchell, M.J. An ionizable lipid toolbox for RNA delivery. *Nat. Commun.* **2021**, *12*, 7233. [CrossRef] [PubMed]
58. Witten, J.; Raji, I.; Manan, R.S.; Beyer, E.; Bartlett, S.; Tang, Y.; Ebadi, M.; Lei, J.; Nguyen, D.; Oladimeji, F.; et al. Artificial intelligence-guided design of lipid nanoparticles for pulmonary gene therapy. *Nat. Biotechnol.* **2024**, *43*, 1790–1799. [CrossRef] [PubMed]
59. Whitley, J.; Zwolinski, C.; Denis, C.; Maughan, M.; Hayles, L.; Clarke, D.; Snare, M.; Liao, H.; Chiou, S.; Marmura, T.; et al. Development of mRNA manufacturing for vaccines and therapeutics: mRNA platform requirements and development of a scalable production process to support early phase clinical trials. *Transl. Res.* **2021**, *242*, 38–55. [CrossRef] [PubMed]
60. Shepherd, S.J.; Warzecha, C.C.; Yadavali, S.; El-Mayta, R.; Alameh, M.-G.; Wang, L.; Weissman, D.; Wilson, J.M.; Issadore, D.; Mitchell, M.J. Scalable mRNA and siRNA Lipid Nanoparticle Production Using a Parallelized Microfluidic Device. *Nano Lett.* **2021**, *21*, 5671–5680. [CrossRef] [PubMed]
61. European Directorate for the Quality of Medicines & HealthCare (EDQM). European Pharmacopoeia Commission Adopts First Three General Texts on mRNA Vaccines (Ph. Eur. General Texts 5.36, 5.39 and 5.40). Council of Europe—European Pharma-Copoeia 11.8. Available online: https://www.edqm.eu/en/-/european-pharmacopoeia-commission-adopts-first-three-general-texts-on-mrna-vaccines (accessed on 13 November 2025).
62. Packer, M.; Gyawali, D.; Yerabolu, R.; Schariter, J.; White, P. A novel mechanism for the loss of mRNA activity in lipid nanoparticle delivery systems. *Nat. Commun.* **2021**, *12*, 6777. [CrossRef] [PubMed]
63. Muramatsu, H.; Lam, K.; Bajusz, C.; Laczkó, D.; Karikó, K.; Schreiner, P.; Martin, A.; Lutwyche, P.; Heyes, J.; Pardi, N. Lyophilization provides long-term stability for a lipid nanoparticle-formulated, nucleoside-modified mRNA vaccine. *Mol. Ther.* **2022**, *30*, 1941–1951. [CrossRef] [PubMed]
64. Crommelin, D.J.; Anchordoquy, T.J.; Volkin, D.B.; Jiskoot, W.; Mastrobattista, E. Addressing the Cold Reality of mRNA Vaccine Stability. *J. Pharm. Sci.* **2021**, *110*, 997–1001. [CrossRef] [PubMed]
65. Driskill, M.M.; Coates, I.A.; Hurst, P.J.; Rajesh, N.U.; Dulay, M.T.; Waymouth, R.M.; Akahata, W.; Matsuda, K.; Smith, J.F.; Jacobson, G.B.; et al. Lyophilized SARS-CoV-2 self-amplifying RNA vaccines for microneedle array patch delivery. *J. Control. Release* **2025**, *384*, 113944. [CrossRef] [PubMed]
66. Gilleron, J.; Querbes, W.; Zeigerer, A.; Borodovsky, A.; Marsico, G.; Schubert, U.; Manygoats, K.; Seifert, S.; Andree, C.; Stöter, M.; et al. Image-based analysis of lipid nanoparticle–mediated siRNA delivery, intracellular trafficking and endosomal escape. *Nat. Biotechnol.* **2013**, *31*, 638–646. [CrossRef] [PubMed]
67. Wittrup, A.; Ai, A.; Liu, X.; Hamar, P.; Trifonova, R.; Charisse, K.; Manoharan, M.; Kirchhausen, T.; Lieberman, J. Visualizing lipid-formulated siRNA release from endosomes and target gene knockdown. *Nat. Biotechnol.* **2015**, *33*, 870–876. [CrossRef] [PubMed]
68. Cheng, Q.; Wei, T.; Farbiak, L.; Johnson, L.T.; Dilliard, S.A.; Siegwart, D.J. Selective organ targeting (SORT) nanoparticles for tissue-specific mRNA delivery and CRISPR–Cas gene editing. *Nat. Nanotechnol.* **2020**, *15*, 313–320. [CrossRef] [PubMed]

69. Billingsley, M.M.; Gong, N.; Mukalel, A.J.; Thatte, A.S.; El-Mayta, R.; Patel, S.K.; Metzloff, A.E.; Swingle, K.L.; Han, X.; Xue, L.; et al. In Vivo mRNA CAR T Cell Engineering via Targeted Ionizable Lipid Nanoparticles with Extrahepatic Tropism. *Small* **2023**, *20*, e2304378. [CrossRef] [PubMed]
70. Kilchrist, K.V.; Dimobi, S.C.; Jackson, M.A.; Evans, B.C.; Werfel, T.A.; Dailing, E.A.; Bedingfield, S.K.; Kelly, I.B.; Duvall, C.L. Gal8 Visualization of Endosome Disruption Predicts Carrier-Mediated Biologic Drug Intracellular Bioavailability. *ACS Nano* **2019**, *13*, 1136–1152. [CrossRef] [PubMed]
71. Paramasivam, P.; Franke, C.; Stöter, M.; Höijer, A.; Bartesaghi, S.; Sabirsh, A.; Lindfors, L.; Arteta, M.Y.; Dahlén, A.; Bak, A.; et al. Endosomal escape of delivered mRNA from endosomal recycling tubules visualized at the nanoscale. *J. Cell Biol.* **2021**, *221*, e202110137. [CrossRef] [PubMed]
72. Verbeke, R.; Hogan, M.J.; Loré, K.; Pardi, N. Innate immune mechanisms of mRNA vaccines. *Immunity* **2022**, *55*, 1993–2005. [CrossRef] [PubMed]
73. Tahtinen, S.; Tong, A.-J.; Himmels, P.; Oh, J.; Paler-Martinez, A.; Kim, L.; Wichner, S.; Oei, Y.; McCarron, M.J.; Freund, E.C.; et al. IL-1 and IL-1ra are key regulators of the inflammatory response to RNA vaccines. *Nat. Immunol.* **2022**, *23*, 532–542. [CrossRef] [PubMed]
74. Alameh, M.G.; Tombácz, I.; Bettini, E.; Lederer, K.; Ndeupen, S.; Sittplangkoon, C.; Wilmore, J.R.; Gaudette, B.T.; Soliman, O.Y.; Pine, M.; et al. Lipid nanoparticles enhance the efficacy of mRNA and protein subunit vaccines by promoting robust antigen presentation and germinal center formation. *Immunity* **2021**, *54*, 2877–2892.e7. [PubMed]
75. Han, X.; Alameh, M.-G.; Butowska, K.; Knox, J.J.; Lundgreen, K.; Ghattas, M.; Gong, N.; Xue, L.; Xu, Y.; Lavertu, M.; et al. Adjuvant lipidoid-substituted lipid nanoparticles augment the immunogenicity of SARS-CoV-2 mRNA vaccines. *Nat. Nanotechnol.* **2023**, *18*, 1105–1114. [CrossRef] [PubMed]
76. Bitounis, D.; Jacquinet, E.; Rogers, M.A.; Amiji, M.M. Strategies to reduce the risks of mRNA drug and vaccine toxicity. *Nat. Rev. Drug Discov.* **2024**, *23*, 281–300. [CrossRef] [PubMed]
77. Pardi, N.; Hogan, M.J.; Naradikian, M.S.; Parkhouse, K.; Cain, D.W.; Jones, L.; Moody, M.A.; Verkerke, H.P.; Myles, A.; Willis, E.; et al. Nucleoside-modified mRNA vaccines induce potent T follicular helper and germinal center B cell responses. *J. Exp. Med.* **2018**, *215*, 1571–1588. [CrossRef] [PubMed]
78. Turner, J.S.; O'halloran, J.A.; Kalaidina, E.; Kim, W.; Schmitz, A.J.; Zhou, J.Q.; Lei, T.; Thapa, M.; Chen, R.E.; Case, J.B.; et al. SARS-CoV-2 mRNA vaccines induce persistent human germinal centre responses. *Nature* **2021**, *596*, 109–113. [CrossRef] [PubMed]
79. Goel, R.R.; Painter, M.M.; Apostolidis, S.A.; Mathew, D.; Meng, W.; Rosenfeld, A.M.; Lundgreen, K.A.; Reynaldi, A.; Khoury, D.S.; Pattekar, A.; et al. mRNA vaccines induce durable immune memory to SARS-CoV-2 and variants of concern. *Science* **2021**, *374*, abm0829. [CrossRef] [PubMed]
80. Liang, F.; Lindgren, G.; Lin, A.; Thompson, E.A.; Ols, S.; Röhss, J.; John, S.; Hassett, K.; Yuzhakov, O.; Bahl, K.; et al. Efficient Targeting and Activation of Antigen-Presenting Cells In Vivo after Modified mRNA Vaccine Administration in Rhesus Macaques. *Mol. Ther.* **2017**, *25*, 2635–2647. [CrossRef] [PubMed]
81. Doria-Rose, N.; Suthar, M.S.; Makowski, M.; O'Connell, S.; McDermott, A.B.; Flach, B.; Ledgerwood, J.E.; Mascola, J.R.; Graham, B.S.; Lin, B.C.; et al. Antibody Persistence through 6 Months after the Second Dose of mRNA-1273 Vaccine for Covid-19. *N. Engl. J. Med.* **2021**, *384*, 2259–2261, Erratum in *N. Engl. J. Med.* **2022**, 386, 500. [CrossRef] [PubMed]
82. Khoury, D.S.; Cromer, D.; Reynaldi, A.; Schlub, T.E.; Wheatley, A.K.; Juno, J.A.; Subbarao, K.; Kent, S.J.; Triccas, J.A.; Davenport, M.P. Neutralizing antibody levels are highly predictive of immune protection from symptomatic SARS-CoV-2 infection. *Nat. Med.* **2021**, *27*, 1205–1211. [CrossRef] [PubMed]
83. Cele, S.; Jackson, L.; Khoury, D.S.; Khan, K.; Moyo-Gwete, T.; Tegally, H.; San, J.E.; Cromer, D.; Scheepers, C.; Amoako, D.; et al. SARS-CoV-2 Omicron has extensive but incomplete escape of Pfizer BNT162b2 elicited neutralization and re-quires ACE2 for infection. *Nature* **2022**, *602*, 654–656. [PubMed]
84. Uraki, R.; Korber, B.; Diamond, M.S.; Kawaoka, Y. SARS-CoV-2 variants: Biology, pathogenicity, immunity and control. *Nat. Rev. Microbiol.* **2025**, *24*, 8–28. [CrossRef] [PubMed]
85. Cao, Y.; Jian, F.; Wang, J.; Yu, Y.; Song, W.; Yisimayi, A.; An, R.; Chen, X.; Zhang, N.; Wang, Y.; et al. Imprinted SARS-CoV-2 humoral immunity induces convergent Omicron RBD evolution. *Nature* **2022**, *614*, 521–529. [CrossRef] [PubMed]
86. Painter, M.M.; Mathew, D.; Goel, R.R.; Apostolidis, S.A.; Pattekar, A.; Kuthuru, O.; Baxter, A.E.; Herati, R.S.; Oldridge, D.A.; Gouma, S.; et al. Rapid induction of antigen-specific CD4+ T cells is associated with coordinated humoral and cellular immunity to SARS-CoV-2 mRNA vaccination. *Immunity* **2021**, *54*, 2133–2142.e3. [CrossRef] [PubMed]
87. Liu, J.; Chandrashekar, A.; Sellers, D.; Barrett, J.; Jacob-Dolan, C.; Lifton, M.; McMahan, K.; Sciacca, M.; VanWyk, H.; Wu, C.; et al. Vaccines elicit highly conserved cellular immunity to SARS-CoV-2 Omicron. *Nature* **2022**, *603*, 493–496. [CrossRef] [PubMed]
88. Muro, R.; Wang, S.; Ito-Kureha, T.; Huynh, H.H.; Kobiyama, K.; Sugita, T.; Okamoto, K.; Nakano, K.; Okamura, T.; Kubo, M.; et al. A distinct antigen presentation pathway drives potent T cell immunity in lipid nanoparticle–based mRNA vaccines. *Sci. Adv.* **2026**, *12*, eaec7827. [CrossRef] [PubMed]

89. Cromer, D.; Steain, M.; Reynaldi, A.; Schlub, T.E.; Wheatley, A.K.; Juno, J.A.; Kent, S.J.; Triccas, J.A.; Khoury, D.S.; Davenport, M.P. Neutralising antibody titres as predictors of protection against SARS-CoV-2 variants and the impact of boosting: A meta-analysis. *Lancet Microbe* **2021**, *3*, e52–e61. [CrossRef] [PubMed]
90. Kiyono, H.; Ernst, P.B. Nasal vaccines for respiratory infections. *Nature* **2025**, *641*, 321–330. [CrossRef] [PubMed]
91. Zhang, H.; Floyd, K.; Fang, Z.; Hoffmann, F.A.; Lee, A.; Froggatt, H.M.; Bharj, G.; Xie, X.; Eppler, H.B.; Santagata, J.M.; et al. Mucosal vaccination in mice provides protection from diverse respiratory threats. *Science* **2026**, *392*, eaea1260. [CrossRef] [PubMed]
92. Suberi, A.; Grun, M.K.; Mao, T.; Israelow, B.; Reschke, M.; Grundler, J.; Akhtar, L.; Lee, T.; Shin, K.; Piotrowski-Daspit, A.S.; et al. Polymer nanoparticles deliver mRNA to the lung for mucosal vaccination. *Sci. Transl. Med.* **2023**, *15*, eabq0603. [CrossRef] [PubMed]
93. Xie, Z.; Lin, Y.-C.; Steichen, J.M.; Ozorowski, G.; Kratochvil, S.; Ray, R.; Torres, J.L.; Liguori, A.; Kalyuzhniy, O.; Wang, X.; et al. mRNA-LNP HIV-1 trimer boosters elicit precursors to broad neutralizing antibodies. *Science* **2024**, *384*, eadk0582. [CrossRef] [PubMed]
94. Schiffner, T.; Phung, I.; Ray, R.; Irimia, A.; Tian, M.; Swanson, O.; Lee, J.H.; Lee, C.-C.D.; Marina-Zárate, E.; Cho, S.Y.; et al. Vaccination induces broadly neutralizing antibody precursors to HIV gp41. *Nat. Immunol.* **2024**, *25*, 1073–1082, Erratum in *Nat. Immunol.* **2024**, *25*, 1307. [CrossRef] [PubMed]
95. Larman, H.B.; Zhao, Z.; Laserson, U.; Li, M.Z.; Ciccia, A.; Gakidis, M.A.M.; Church, G.M.; Kesari, S.; LeProust, E.M.; Solimini, N.L.; et al. Autoantigen discovery with a synthetic human peptidome. *Nat. Biotechnol.* **2011**, *29*, 535–541. [CrossRef] [PubMed]
96. Xu, G.J.; Kula, T.; Xu, Q.; Li, M.Z.; Vernon, S.D.; Ndung'u, T.; Ruxrungtham, K.; Sanchez, J.; Brander, C.; Chung, R.T.; et al. Comprehensive serological profiling of human populations using a synthetic human virome. *Science* **2015**, *348*, aaa0698. [CrossRef] [PubMed]
97. Shrock, E.; Fujimura, E.; Kula, T.; Timms, R.T.; Lee, I.-H.; Leng, Y.; Robinson, M.L.; Sie, B.M.; Li, M.Z.; Chen, Y.; et al. Viral epitope profiling of COVID-19 patients reveals cross-reactivity and correlates of severity. *Science* **2020**, *370*, eabd4250. [CrossRef] [PubMed]
98. Goswami, J.; Cardona, J.F.; Caso, J.; Hsu, D.C.; Simorellis, A.K.; Wilson, L.; Dhar, R.; Wang, X.; Kapoor, A.; Collins, A.; et al. Safety, Tolerability, and Immunogenicity of Revaccination With mRNA-1345, an mRNA Vaccine Against RSV, Administered 12 Months Following a Primary Dose in Adults Aged ≥50 Years. *Clin. Infect. Dis.* **2025**, *82*, e855–e862. [CrossRef] [PubMed]
99. Soens, M.; Ananworanich, J.; Hicks, B.; Lucas, K.J.; Cardona, J.; Sher, L.; Livermore, G.; Schaefers, K.; Henry, C.; Choi, A.; et al. A phase 3 randomized safety and immunogenicity trial of mRNA-1010 seasonal influenza vaccine in adults. *Vaccine* **2025**, *50*, 126847. [CrossRef] [PubMed]
100. Kaplonek, P.; Vargas, R.; Lee, J.S.-L.; Bertera, H.; Astley, E.; Girard, B.; Oostendorp, J.; Henry, C.; Paris, R.; Yu, W.-H.; et al. mRNA-1010 influenza vaccine elicits distinct and enhanced humoral immunity compared to adjuvanted inactivated vaccines. *npj Vaccines* **2025**, *11*, 19. [CrossRef] [PubMed]
101. Spergel, A.K.R.; Ananworanich, J.; Guo, R.; Deng, W.; Carmona, L.; Schaefers, K.; Paila, Y.D.; Kandinov, B.; Eger, C.H.; Sinkiewicz, M.; et al. mRNA-based seasonal influenza and SARS-CoV-2 multicomponent vaccine in healthy adults: A phase 1/2 trial. *Nat. Med.* **2025**, *31*, 1484–1493. [CrossRef] [PubMed]
102. Rudman Spergel, A.K.; Wu, I.; Deng, W.; Cardona, J.; Johnson, K.; Espinosa-Fernandez, I.; Sinkiewicz, M.; Urdaneta, V.; Carmona, L.; Schaefers, K.; et al. Immunogenicity and safety of influenza and COVID-19 multicomponent vaccine in adults ≥50 years: A randomized clinical trial. *JAMA* **2025**, *333*, 1977–1987. [PubMed]
103. Mallory, K.L.; Taylor, J.A.; Zou, X.; Waghela, I.N.; Schneider, C.G.; Sibilo, M.Q.; Punde, N.M.; Perazzo, L.C.; Savransky, T.; Sedegah, M.; et al. Messenger RNA expressing PfCSP induces functional, protective immune responses against malaria in mice. *npj Vaccines* **2021**, *6*, 84. [CrossRef] [PubMed]
104. Pardi, N.; Secreto, A.J.; Shan, X.; Debonera, F.; Glover, J.; Yi, Y.; Muramatsu, H.; Ni, H.; Mui, B.L.; Tam, Y.K.; et al. Administration of nucleoside-modified mRNA encoding broadly neutralizing antibody protects humanized mice from HIV-1 challenge. *Nat. Commun.* **2017**, *8*, 14630. [CrossRef] [PubMed]
105. Mevorach, D.; Anis, E.; Cedar, N.; Bromberg, M.; Haas, E.J.; Nadir, E.; Olsha-Castell, S.; Arad, D.; Hasin, T.; Levi, N.; et al. Myocarditis after BNT162b2 mRNA Vaccine against Covid-19 in Israel. *N. Engl. J. Med.* **2021**, *385*, 2140–2149. [CrossRef] [PubMed]
106. Oster, M.E.; Shay, D.K.; Su, J.R.; Gee, J.; Creech, C.B.; Broder, K.R.; Edwards, K.; Soslow, J.H.; Dendy, J.M.; Schlaudecker, E.; et al. Myocarditis Cases Reported After mRNA-Based COVID-19 Vaccination in the US From December 2020 to August 2021. *JAMA* **2022**, *327*, 331–340. [CrossRef] [PubMed]
107. Patone, M.; Mei, X.W.; Handunnetthi, L.; Dixon, S.; Zaccardi, F.; Shankar-Hari, M.; Watkinson, P.; Khunti, K.; Harnden, A.; Coupland, C.A.C.; et al. Risks of myocarditis, pericarditis, and cardiac arrhythmias associated with COVID-19 vaccination or SARS-CoV-2 infection. *Nat. Med.* **2021**, *28*, 410–422. [CrossRef] [PubMed]

108. Bozkurt, B.; Kamat, I.; Hotez, P.J. Myocarditis with COVID-19 mRNA vaccines. *Circulation* **2021**, *144*, 471–484. [CrossRef] [PubMed]
109. Shimabukuro, T.T.; Cole, M.; Su, J.R. Reports of Anaphylaxis After Receipt of mRNA COVID-19 Vaccines in the US—December 14, 2020-January 18, 2021. *JAMA* **2021**, *325*, 1101–1102. [CrossRef] [PubMed]
110. Yang, Q.; Lai, S.K. Anti-PEG immunity: Emergence, characteristics, and unaddressed questions. *Wiley Interdiscip. Rev. Nanomed. Nanobiotechnol.* **2015**, *7*, 655–677. [PubMed]
111. Ju, Y.; Lee, W.S.; Pilkington, E.H.; Kelly, H.G.; Li, S.; Selva, K.J.; Wragg, K.M.; Subbarao, K.; Nguyen, T.H.O.; Rowntree, L.C.; et al. Anti-PEG Antibodies Boosted in Humans by SARS-CoV-2 Lipid Nanoparticle mRNA Vaccine. *ACS Nano* **2022**, *16*, 11769–11780. [CrossRef] [PubMed]
112. Kozma, G.T.; Shimizu, T.; Ishida, T.; Szebeni, J. Anti-PEG antibodies: Properties, formation, testing and role in adverse immune reactions to PEGylated nano-biopharmaceuticals. *Adv. Drug Deliv. Rev.* **2020**, *154–155*, 163–175. [CrossRef] [PubMed]
113. Shimabukuro, T.T.; Kim, S.Y.; Myers, T.R.; Moro, P.L.; Oduyebo, T.; Panagiotakopoulos, L.; Marquez, P.L.; Olson, C.K.; Liu, R.; Chang, K.T.; et al. Preliminary Findings of mRNA Covid-19 Vaccine Safety in Pregnant Persons. *N. Engl. J. Med.* **2021**, *384*, 2273–2282. [CrossRef] [PubMed]
114. Gray, K.J.; Bordt, E.A.; Atyeo, C.; Deriso, E.; Akinwunmi, B.; Young, N.; Baez, A.M.; Shook, L.L.; Cvrk, D.; James, K.; et al. COVID-19 vaccine response in pregnant and lactating women: A cohort study. *Am. J. Obstet. Gynecol.* **2021**, *225*, 303.e1–303.e17. [CrossRef] [PubMed]
115. Nogueira, S.S.; Schlegel, A.; Maxeiner, K.; Weber, B.; Barz, M.; Schroer, M.A.; Blanchet, C.E.; Svergun, D.I.; Ramishetti, S.; Peer, D.; et al. Polysarcosine-Functionalized Lipid Nanoparticles for Therapeutic mRNA Delivery. *ACS Appl. Nano Mater.* **2020**, *3*, 10634–10645. [CrossRef]
116. Jackson, N.A.C.; Kester, K.E.; Casimiro, D.; Gurunathan, S.; DeRosa, F. The promise of mRNA vaccines: A biotech and industrial perspective. *npj Vaccines* **2020**, *5*, 11. [CrossRef] [PubMed]
117. Saville, M.; Cramer, J.P.; Downham, M.; Hacker, A.; Lurie, N.; Van der Veken, L.; Whelan, M.; Hatchett, R. Delivering Pandemic Vaccines in 100 Days—What Will It Take? *N. Engl. J. Med.* **2022**, *387*, E3. [CrossRef] [PubMed]
118. Mwila, C.; Ekström, A.M.; Kampmann, B.; Peterson, S.S.; Alexander, N.; Dereje, N.; Bayih, A.G.; Kaseya, J.; Ottersen, O.P. Operationalizing African self-reliance in vaccine manufacturing. *Glob. Health Action* **2025**, *18*, 2560209. [CrossRef] [PubMed]

Disclaimer/Publisher's Note: The statements, opinions and data contained in all publications are solely those of the individual author(s) and contributor(s) and not of MDPI and/or the editor(s). MDPI and/or the editor(s) disclaim responsibility for any injury to people or property resulting from any ideas, methods, instructions or products referred to in the content.